

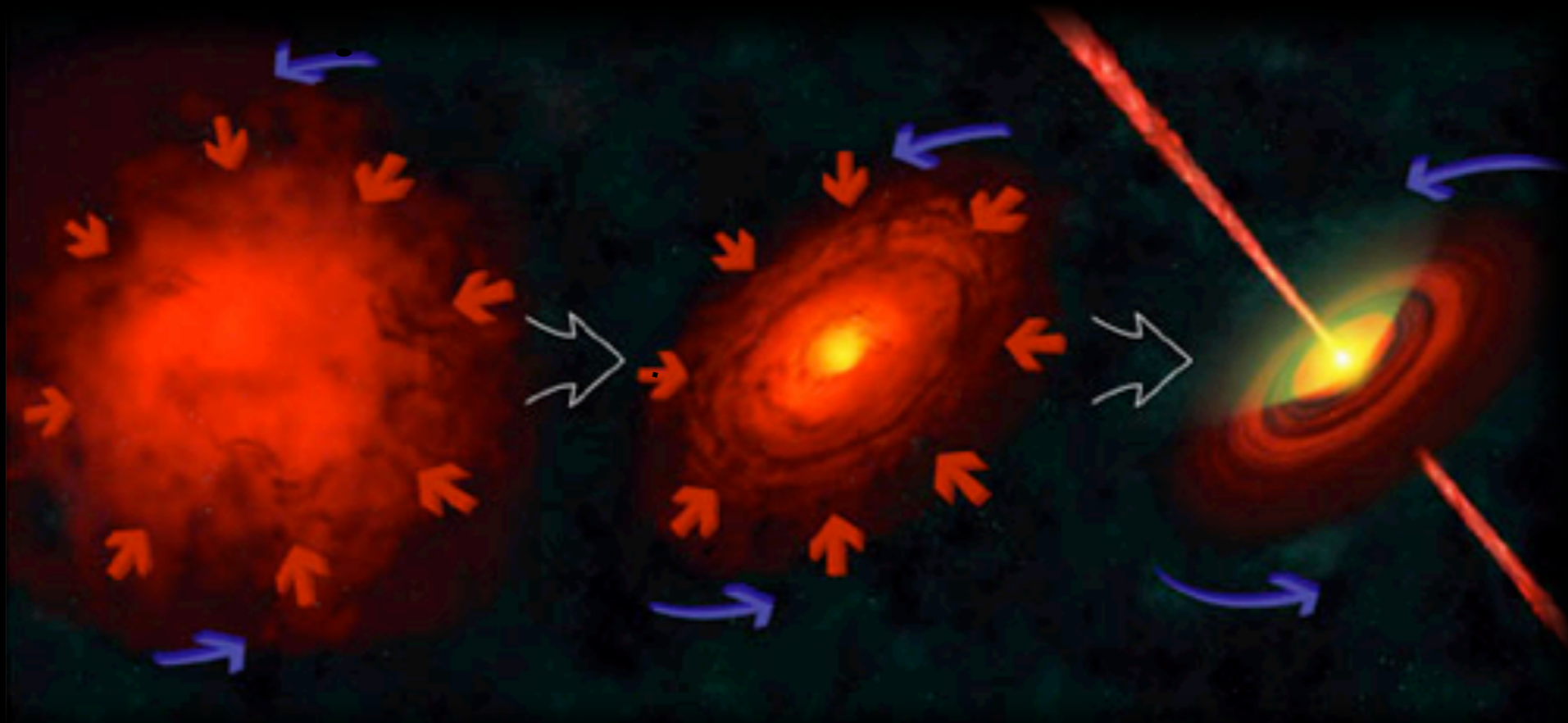
An Observer's View of Galactic Star Formation



Alyssa A. Goodman
Harvard-Smithsonian Center for Astrophysics

image courtesy of Nimesh Patel (Sierra Nevada Optical Observatory from the 30-m)

Star Formation 101



©Adison-Wesley 2004

Jeans Fragmentation

leads to **Accretion Disks**

+ **Jets** to get rid of angular momentum

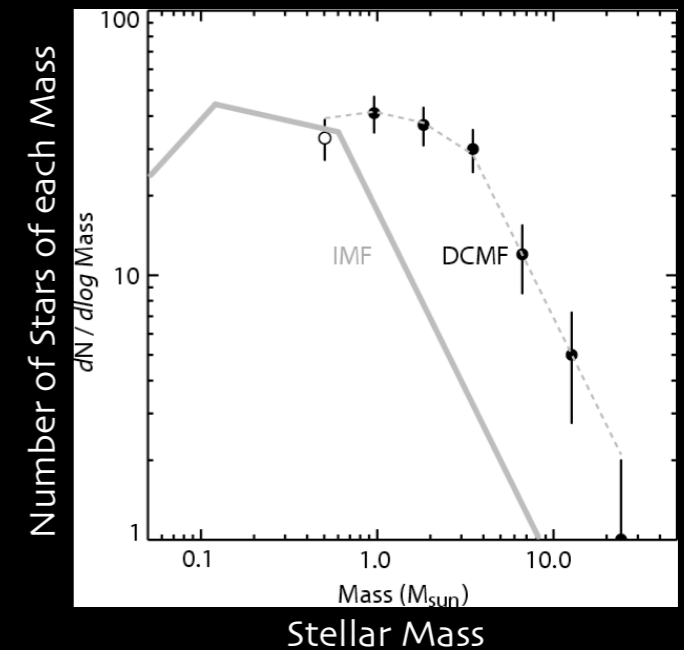
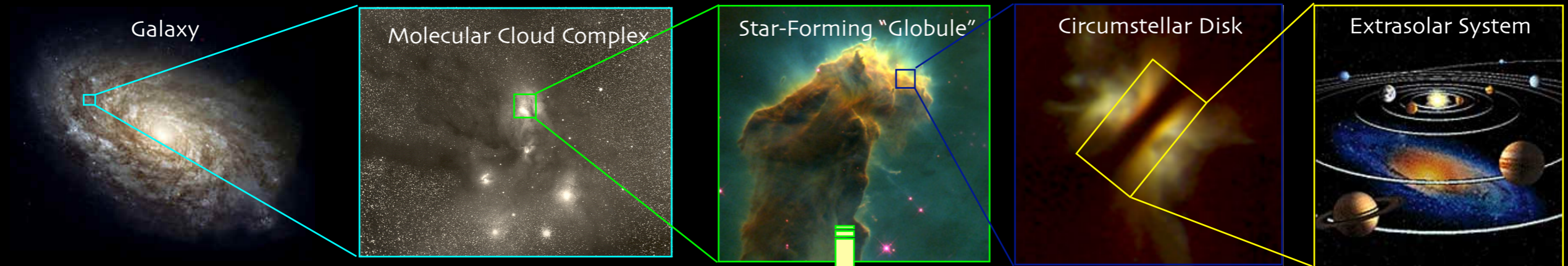
Why does this fail on large scales? (Hierarchical “initial conditions,” plus $t_{\text{ff}} \approx t_{\text{cross}} \approx t_{\text{Jeans}}$.)

$$M_J = \frac{1}{8} \left(\frac{\pi k T}{G \mu} \right)^{3/2} \frac{1}{\rho^{1/2}} \propto \frac{T^{3/2}}{\rho^{1/2}}$$

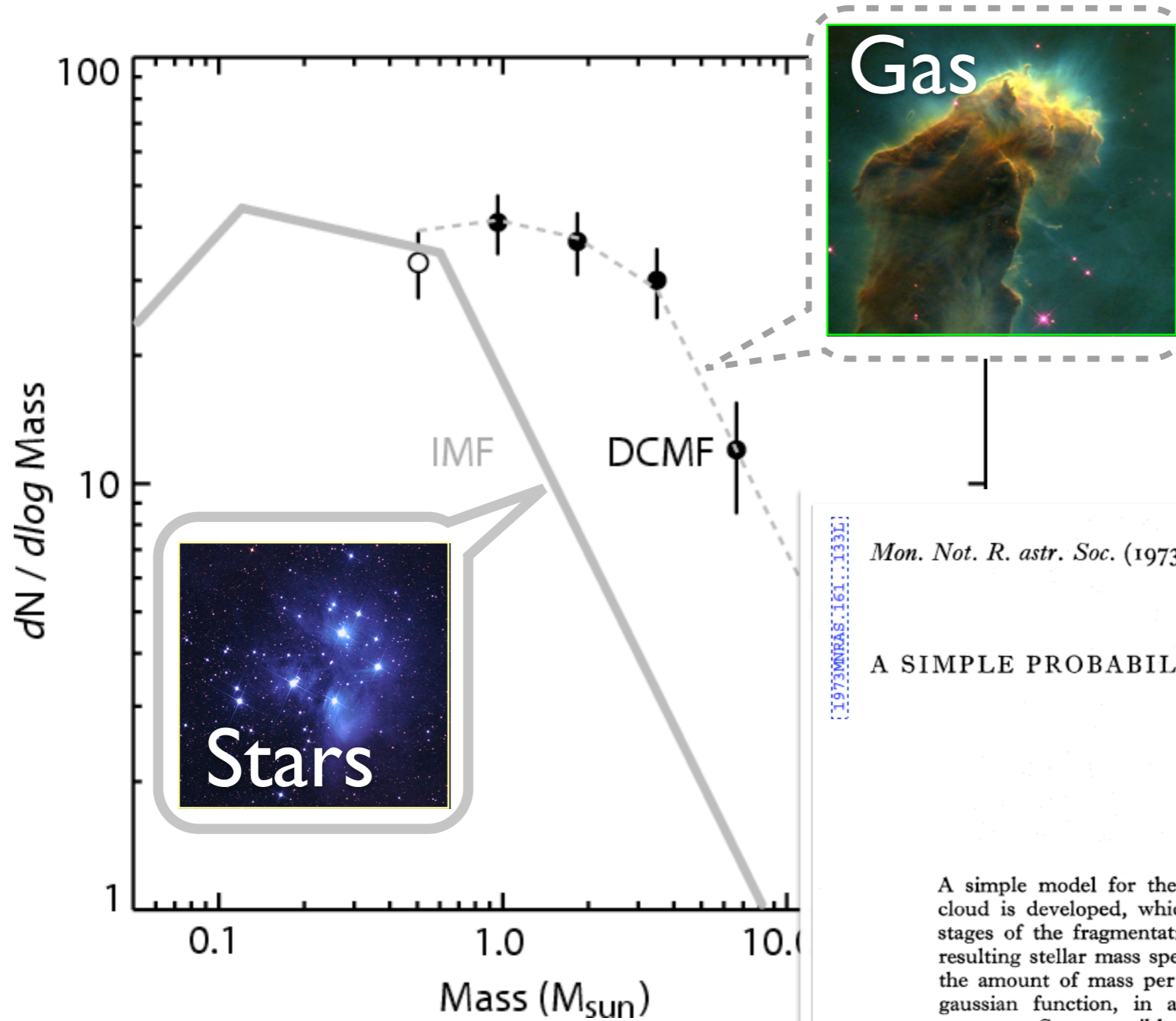
$$10K, 2.33 \text{amu}, n_H = 2 \times 10^5 \text{cm}^{-3} \rightarrow 2M_\odot$$

$$50K, 2.33 \text{amu}, n_H = 200 \text{cm}^{-3} \rightarrow 700M_\odot$$

Star (and Planet, and Moon) Formation 201



“CMF” “IMF”??



[1973MNRAS...161..133L](#)
Mon. Not. R. astr. Soc. (1973) **161**, 133–143.

A SIMPLE PROBABILISTIC THEORY OF FRAGMENTATION

Richard B. Larson

(Received 1972 October 5)

SUMMARY

A simple model for the fragmentation process in a collapsing interstellar cloud is developed, which is based on the assumption that the successive stages of the fragmentation process can be treated as random events. The resulting stellar mass spectrum predicted by the model, defined in terms of the amount of mass per unit logarithmic mass interval, is approximately a gaussian function, in agreement with the empirical initial stellar mass spectrum. Some possible ways of accounting for differences in the initial mass spectrum between different stellar systems are also discussed.

Alves, Lombardi & Lada 2007

*Magnetic
Fields*

Gravity

*Chemical & Phase
Transformations*

~ 1 pc

Star (& Planet) Formation 301

Radiation

*Thermal
Pressure*

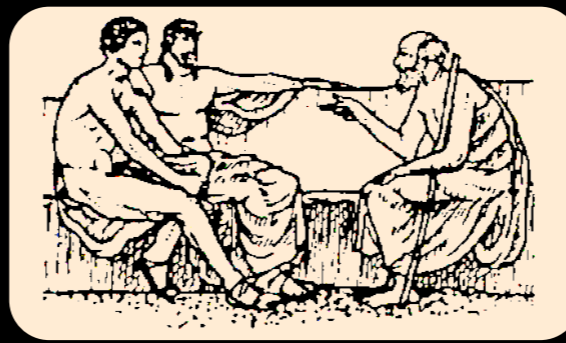
“Turbulence”

(Random Kinetic Energy)

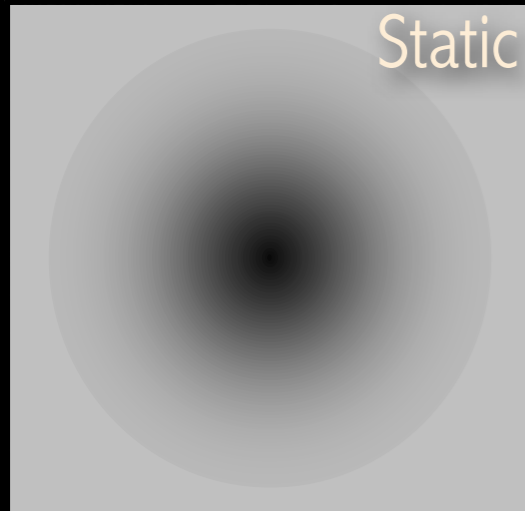
*Outflows
& Winds*

Image Credit: Foster et al. 2012, CfA/COMPLETE Deep Megacam Image of West End of Perseus

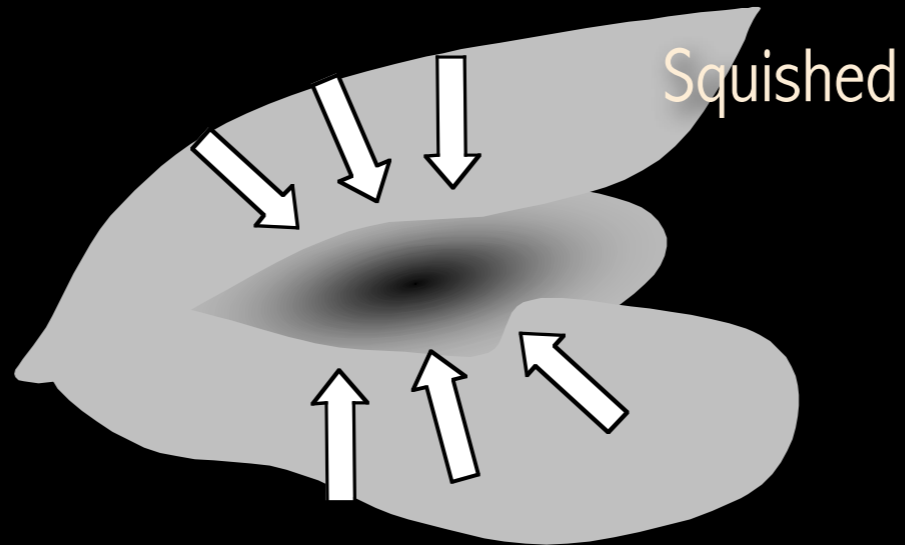
“Modernist”



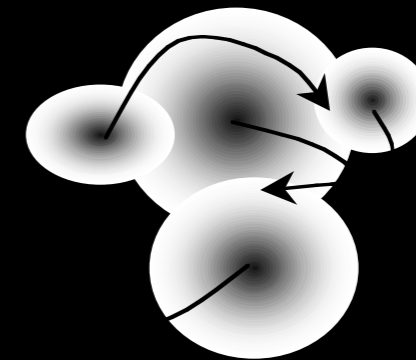
Philosophy



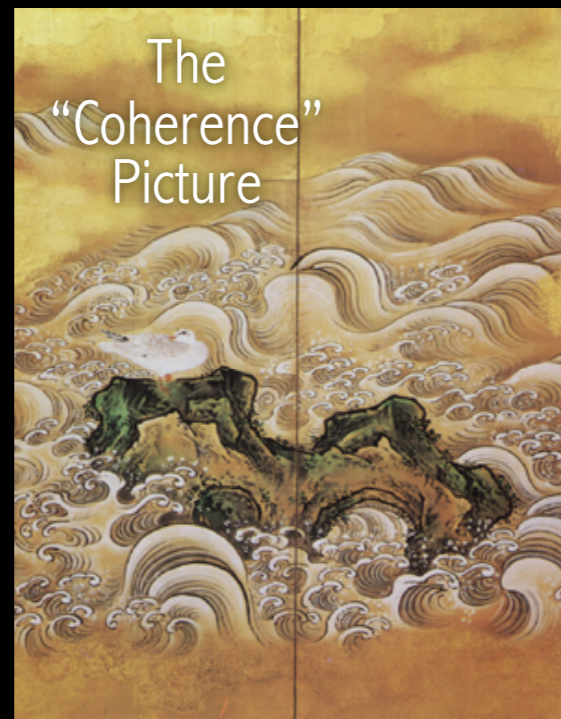
Static



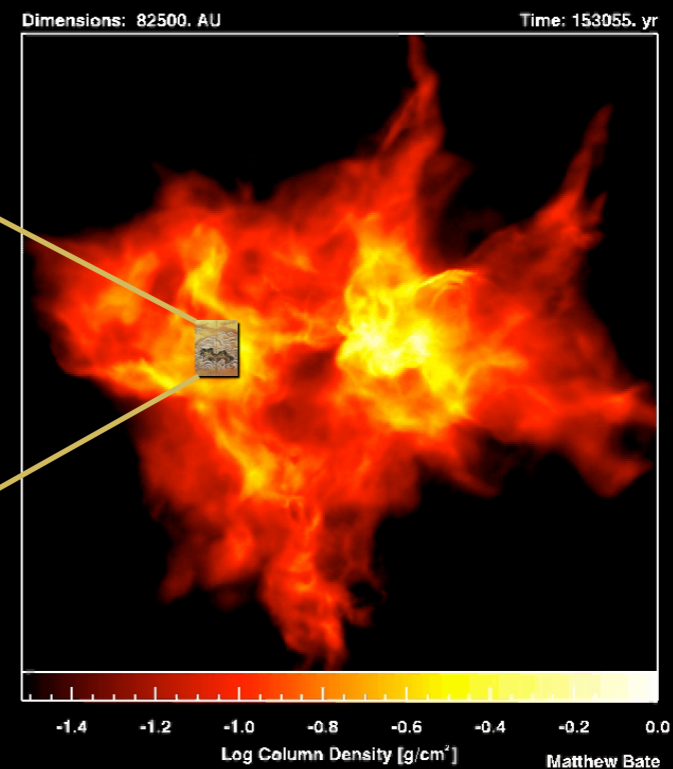
Squished



Competitive
Accretion



The
“Coherence”
Picture



Astronomy Dataserve Network

theastrodata.org/dvn/

Search Twitter | Related Tweets | Trending: ...

CfA HARVARD-SMITHSONIAN CENTER FOR ASTROPHYSICS EXPLORING THE UNIVERSE

POWERED BY THE **Dataserve Network** PROJECT v. 3.2

Create Account | Log In

Astronomy Dataserve Network

This is the Astronomy data repository for Harvard affiliates. The project is the Seamless Astronomy group at the Harvard-Smithsonian Center for Astrophysics, the Wolbach Library, and IQSS with support from the FAS Science Resource Center.

Released Dataserves

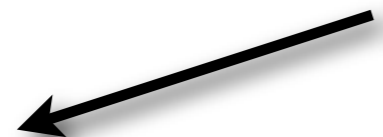
Dataserves: 6 | Studies: 69 | Files: 554

Name	View Info [+]	Harvard-S
CfA Library Datasets	View Info [+]	Harvard-S
theastrodata	View Info [+]	Harvard-S
Soderberg, Alicia		Harvard U
Astroinformatics of galaxies & quasars	View Info [+]	Harvard-S
COMPLETE	View Info [+]	Harvard-S
1.2 Meter CO Survey	View Info [+]	Smithson

About | Research | Education & Outreach | Faculty

HARVARD-SMITHSONIAN CENTER FOR ASTROPHYSICS

Also an "observatory"



NASA/IPAC Infrared Science Archive
for NASA's Infrared and Submillimeter Data

IRSA

Home About Holdings Missions Documentation Helpdesk

C2D Spitzer and Ancillary Data

You can get a close-up map of a region by clicking on any blue, red, green or yellow overlays on the above image, or by typing a coordinate below. Spitzer instrument color code: **IRAC** -- blue, **MIPS** -- red, **IRS** -- green, **BOLOCAM** -- yellow.

image courtesy of Nimesh Patel (Sierra Nevada Optical Observatory from the 30-m)

x-ray Chandra (PMS census, hot gas)

uv FUSE, GALEX (hot young stars, spectra, accretion measures)

optical HST + much glass-on-ground! (nebular imaging, spectroscopy of stars & gas, extinction mapping, B-field maps, stellar & jet motions)

near-IR primarily glass-on-ground (imaging & spectroscopy "through" dust, extinction mapping, B-field maps, AO disks, stellar & jet motions)

mid-IR Spitzer, WISE (dust imaging, young star SEDs, star formation rates)

far-IR IRAS, Spitzer, Herschel, SOFIA (dust imaging, SEDs, dust properties)

sub-mm Herschel, SMA, ALMA (gas kinematics & properties, dust imaging (including disks), young source counting)

mm FCRAO, Mopra, CfA mini, ALMA, CARMA, IRAM 30-m, PdB: (gas kinematics & properties, young source counting, large-scale gas distribution, B-field via Zeeman and polarimetry)

cm GBT, VLA, JVLA, VLBA, Effelsberg (gas kinematics & properties, maser motions, B-field via Zeeman and polarimetry)

But, we can (almost) **never** observe...

time scales >> human lifetime

three spatial dimensions

So...

we count things \longleftrightarrow “statistics”

we make up stories \longleftrightarrow “Bayesian statistics”

Click here to see all papers in this table, together in an ADS Private library	largest size scale traced (pc)	sample historic reference	sample modern reference	learn more	even more
measuring galactic star formation rate	10000	1978 Smith, Biermann & Mezger	2010 Robitaille & Whitney	2009 Evans et al.	
detection of HI in ISM	5000	1951 Ewen & Purcell	GALFA HI	History	
detection of CO in ISM	5000	1970 Wilson, Jefferts & Penzias	2001 Dame, Hartmann & Thaddeus	cf. FCRAO & Mopra surveys	
temperature mapping	5000	1976 Fazio et al.	2005 Schnee et al.	2012 Kelly et al.	
CO as proxy for column density	500	1982 Frerking, Langer & Wilson	2009 Goodman et al.		
“infrared dark clouds”	300	1998 Carey	2006 Rathborne, Jackson & Simon		
optical/near-IR extinction mapping	100	1919 Barnard	2001 Alves, Lada & Lada		
magnetic field strength	100	1988 Myers & Goodman	2010 Crutcher et al.		
magnetic field morphology	100	1976 Vrba, Strom & Strom	2011 Chapman et al.	2012 Davidson et al.	
spatial & kinematic structure of clouds	50	1975 Encrenaz, Falgarone & Lucas	2008 Goldsmith et al.	2009 Goodman et al.	
bipolar outflows	10	1980 Snell, Loren & Plambeck	2010 Arce et al.	2007 Zhang et al.	
spherical shells	10	1975 Castor, McCray & Weaver	2011 Arce et al.		
“Cloudshine” (scattered light mapping)	10	1970 Matilla	2006 Foster & Goodman	2010 Steinacker et al.	
young source/star censuses (multi- <input type="checkbox"/>)	10	1978 Elias	2009 Evans et al.		
long(er), skinni(er) filaments in dark clouds	10	1919 Barnard	2010 André et al.		
astrochemistry, depletion	1	1999 Caselli et al.	2012 Fontani et al.	1997 Bergin & Langer	
“Clump Mass Functions” (CMF)	1	1994 Williams, de Geus & Blitz	2007 Alves, Lombardi & Lada	1998 Motte, André & Neri	2009 Pineda, Rosolowsky & Goodman
dominance of clusters	1	1991 Lada et al.	2009 Gutermuth et al.	2003 Lada & Lada	
evolutionary sequences (outflows)	1	1983 Bally & Lada	2006 Arce & Sargent	astrobites, Plunkett	
motion of “cores”	1	1975 Dickman	2010 Kirk et al.		
photon-dominated regions	1	1977 Black & Dalgarno	2009 Visser, Van Dischoeck & Black	1995 Sternberg & Dalgarno	1978 Draine
(ultra) compact HII Regions	0.5	1989 Wood & Churchwell	2009 Urquhart et al.		
“NH3” cores (starfull, starless)	0.1	1983 Myers & Benson	2008 Rosolowsky et al.	2009 Foster et al.	
core kinematics (rotation)	0.1	1993 Goodman et al.	2012 Tobin et al.		
core kinematics (infall)	0.1	1995 Myers et al.	2007 Joregensen et al.	1998 Tafalla et al.	
core density profiles	0.1	2001 Alves, Lada & Lada	2011 Pineda et al.	2010 Schnee et al.	2012 Nielbock et al.
filament/core kinematics (coherence)	0.1	1998 Goodman et al.	2010 Pineda et al.	2011 Hacar & Tafalla	
adaptive optics, multiplicity	0.01	1993 Ghez, Neugebauer & Matthews	2012 King et al.		
(3D) motions of masers & young stars	0.01	1968 Lesh	2012 Rygl et al.	2004 Goodman & Arce	
“hot” cores in massive-star forming regions	0.01	1988 Keto, Ho & Haschick	2009 Zhang et al.		
SED-based “disk” evolution models	0.005	1987 Adams, Lada & Shu	2006 Robitaille et al.	2012 Offner et al.	
interferometer “disks”, disk holes (lower-mass)	0.005	1991 Beckwith & Sargent	2009 Carrasco-González et al.	2002 Wilner et al.	
prevalence of disks	0.005	1990 Beckwith et al.	2009 Evans et al.		
accretion(?) “disks” around massive stars	0.001	1988 Keto, Ho & Haschick	2012 Beuther, Linz & Henning		
VELLOs--First Cores	0.0001	2005 Kauffmann et al.	2011 Pineda et al.	1969 Larson	
Pre-Stellar IMF (Luminosity-->Mass)	1E-08	2002 Muench et al.	2012 Da Rio et al.	1999 Luhman et al.	
grain growth, reddening laws, ices	1E-18	1977 Cohen	2012 Foster et al.		

What was I thinking?!



ry ——— Simulation



Images ——— Spectra ——— Counting

SEDs

Classification ——— Cataloging

Theory

Simulation

Images

Spectra

Counting

SEDs

Classification

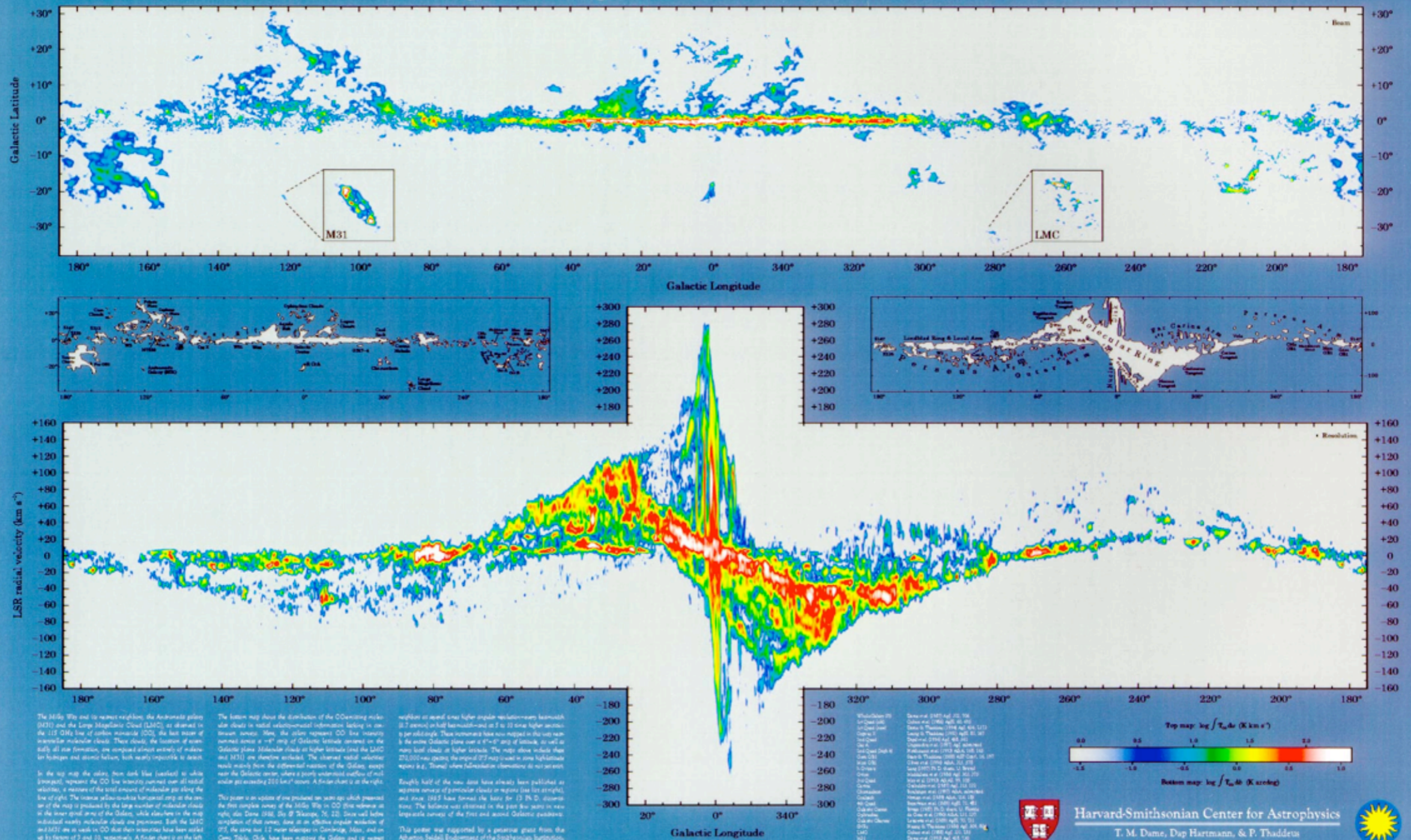
Cataloging



Images + Spectra

Dame et al. 2001

The Milky Way in Molecular Clouds



Larson's "Suggestions"



1981MNRAS.194..809L

Mon. Not. R. astr. Soc. (1981) **194**, 809–826

Turbulence and star formation in molecular clouds

Richard B. Larson *Yale University Observatory, Box 6666, New Haven, Connecticut 06511, USA*

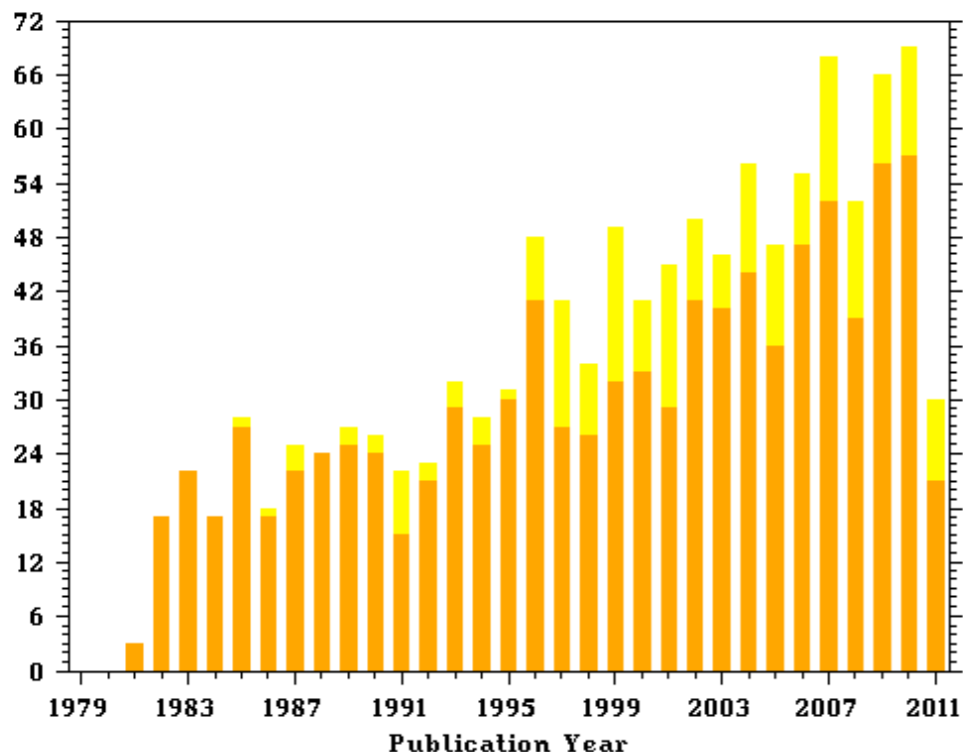
Received 1980 July 7; in original form 1980 May 7

Summary. Data for many molecular clouds and condensations show that the internal velocity dispersion of each region is well correlated with its size and mass, and these correlations are approximately of power-law form. The dependence of velocity dispersion on region size is similar to the Kolmogoroff law for subsonic turbulence, suggesting that the observed motions are all part of a common hierarchy of interstellar turbulent motions. The regions studied are mostly gravitationally bound and in approximate virial equilibrium. However, they cannot have formed by simple gravitational collapse, and it appears likely that molecular clouds and their substructures have been created at least partly by processes of supersonic hydrodynamics. The hierarchy of subcondensations may terminate with objects so small that their internal motions are no longer supersonic; this predicts a minimum protostellar mass of the order of a few tenths of a solar mass. Massive ‘protostellar’ clumps always have supersonic internal motions and will therefore develop complex internal structures, probably leading to the formation of many pre-stellar condensation nuclei that grow by accretion to produce the final stellar mass spectrum. Molecular clouds must be transient structures, and are probably dispersed after not much more than 10^7 yr.

1 Introduction

There is much evidence that stars form in the interiors of dense, gravitationally bound molecular clouds, but little is yet known about the detailed internal structure and dynamics of such clouds, or about the processes by which stars form in them. This lack of direct information has allowed theorists considerable scope for calculating idealized models for the collapse and fragmentation of gas clouds, starting with simple assumed initial conditions (see the reviews by Larson 1977a; Woodward 1978; Bodenheimer & Black 1978). Much of this work has been motivated by the ‘gravitational instability’ picture of star formation elaborated by Jeans (1929), Hoyle (1953) and Hunter (1967), whereby diffuse clouds that are initially nearly uniform collapse and fragment into a hierarchy of successively smaller condensations as the density rises and the Jeans mass decreases.

Citations/Publication Year for 1981MNRAS.194..809L



“Line width - size” $\sigma \sim R^{0.38}$

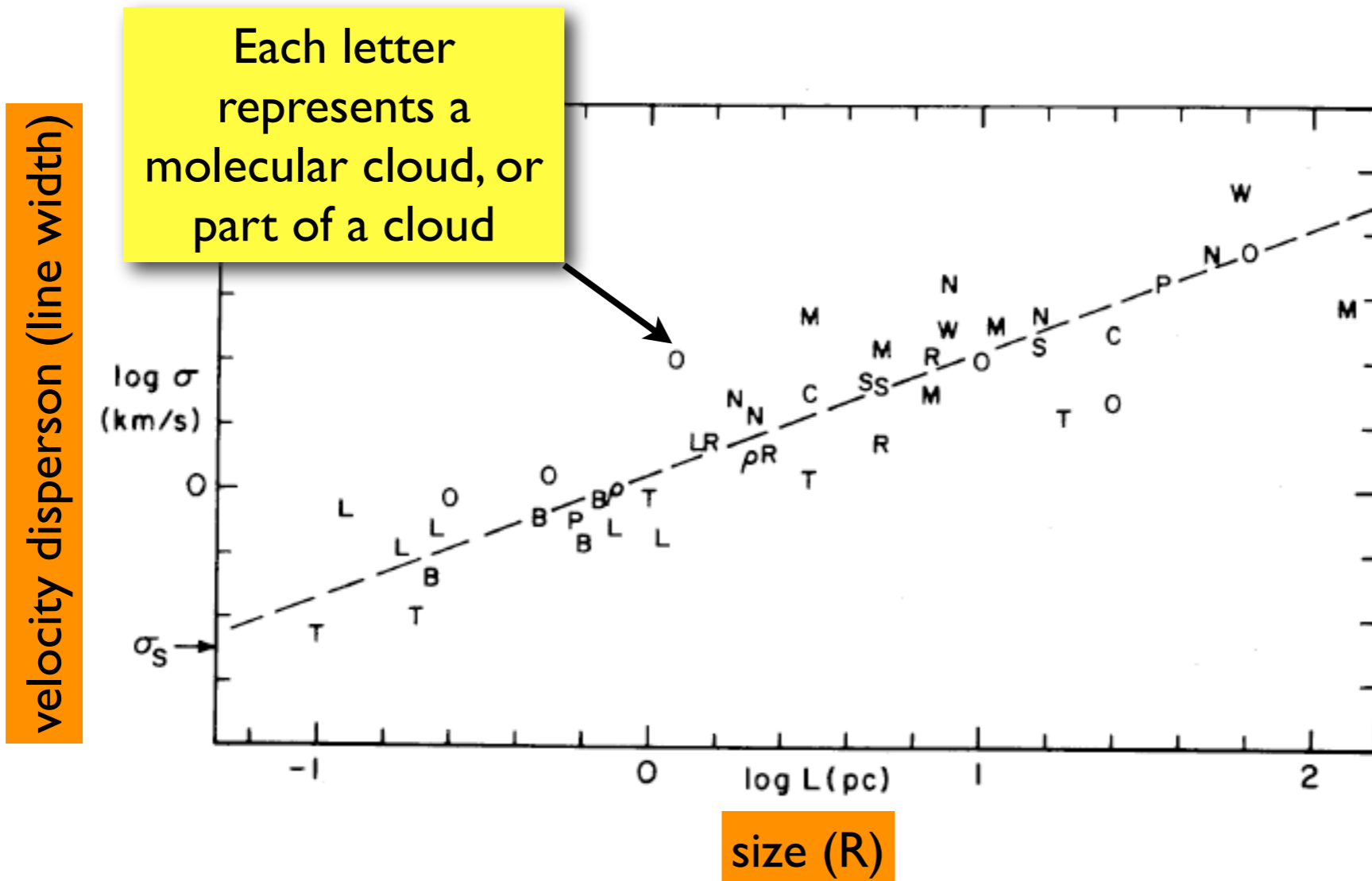


Figure 1. The three-dimensional internal velocity dispersion σ plotted versus the maximum linear dimension L of molecular clouds and condensations, based on data from Table 1; the symbols are identified in Table 1. The dashed line represents equation (1), and σ_s is the thermal velocity dispersion.

More recently, 0.38 has become ~ 0.5 . Larson liked 0.38 because Kolmogorov (incompressible) turbulence would give 0.33. A higher value is consistent with compressible (e.g. “Burger’s” turbulence.)

~100% Correct, but Details have Taken 30 Years (so far)



Summary. Data for many molecular clouds and condensations show that the internal velocity dispersion of each region is well correlated with its size and mass, and these correlations are approximately of power-law form. The dependence of velocity dispersion on region size is similar to the Kolmogoroff law for subsonic turbulence, suggesting that the observed motions are all part of a common hierarchy of interstellar turbulent motions. The regions studied are





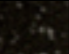
How
appe
at least partly by processes of supersonic hydrodynamics. The hierarchy of subcondensations may terminate with objects so small that their internal motions are no longer supersonic; this predicts a minimum protostellar mass of the order of a few tenths of a solar mass. Massive 'protostellar' clumps always have supersonic internal motions and will therefore develop complex internal structures, probably leading to the formation of many pre-stellar condensation nuclei that grow by accretion to produce the final stellar mass spectrum. Molecular clouds must be transient structures, and are probably dispersed after not much more than 10^7 yr.

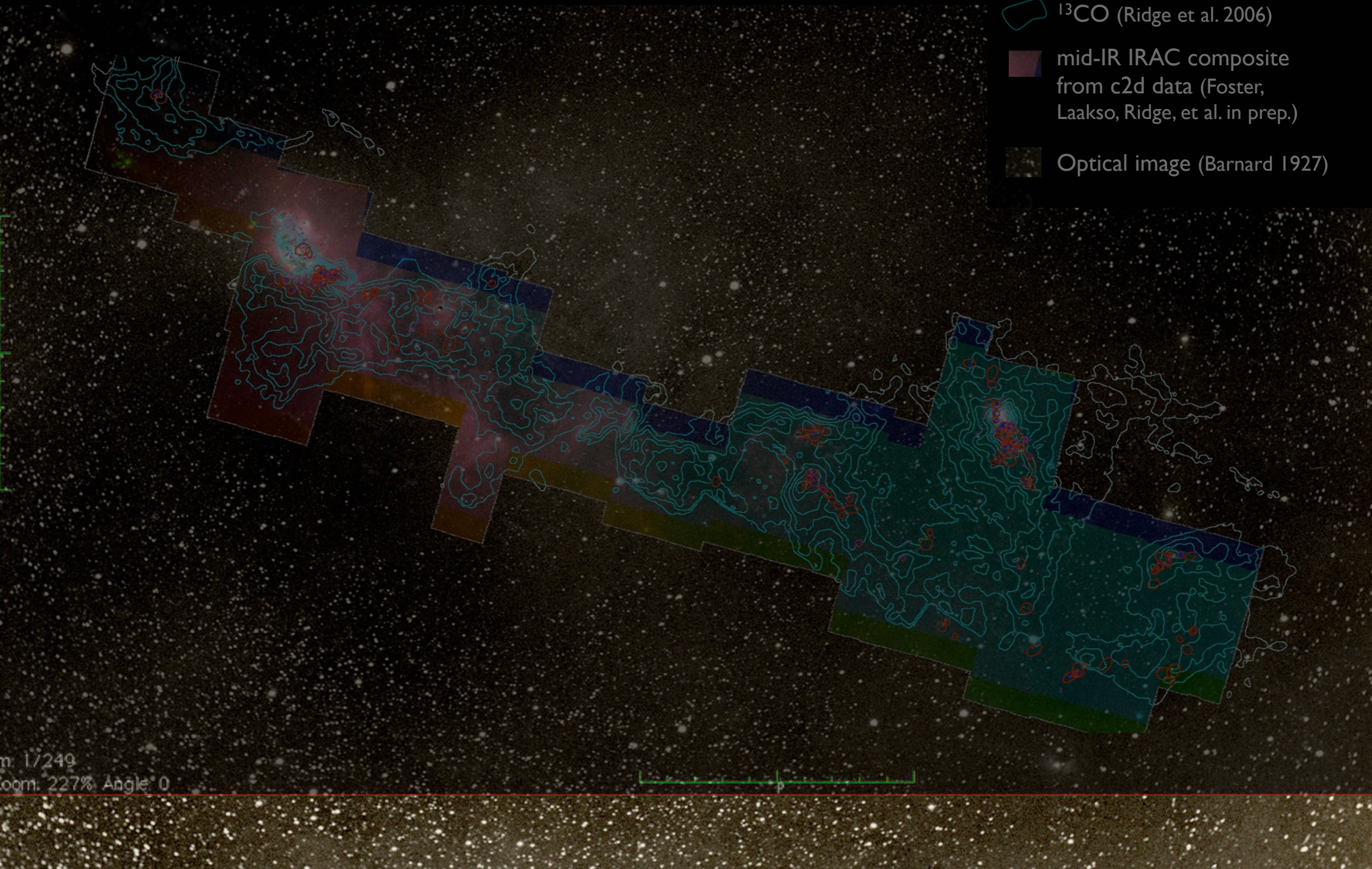
Source/governors of the supersonic motions?

magnetic fields, outflows/winds, SNe, galaxy-scale effects

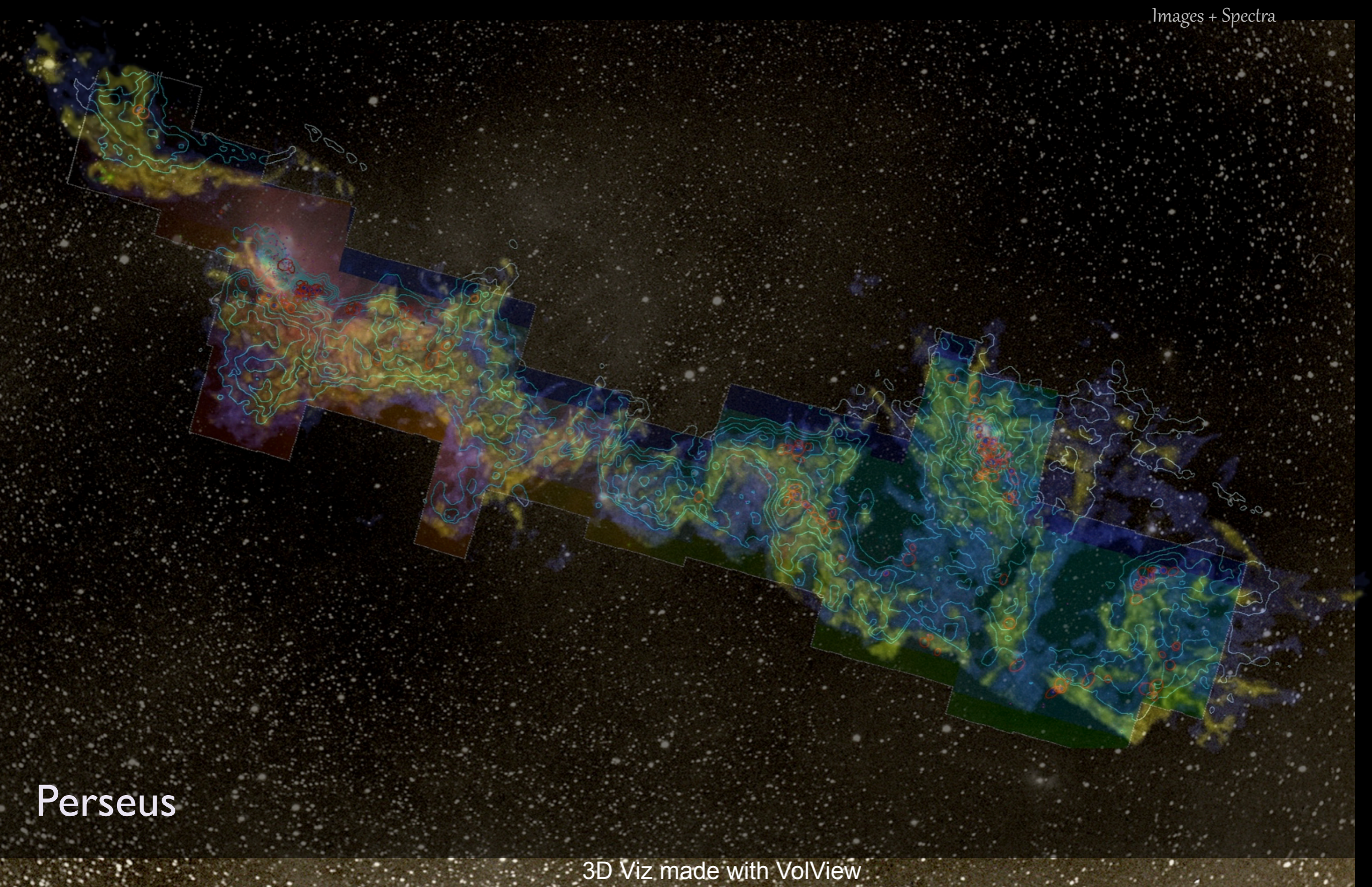
COMPLETE Perseus

Image size: 1305 x 733
WL: 63 WW: 127

-  mm peak (Enoch et al. 2006)
-  sub-mm peak (Hatchell et al. 2005, Kirk et al. 2006)
-  ^{13}CO (Ridge et al. 2006)
-  mid-IR IRAC composite from c2d data (Foster, Laakso, Ridge, et al. in prep.)
-  Optical image (Barnard 1927)



m: 1/249
Zoom: 227% Angle: 0



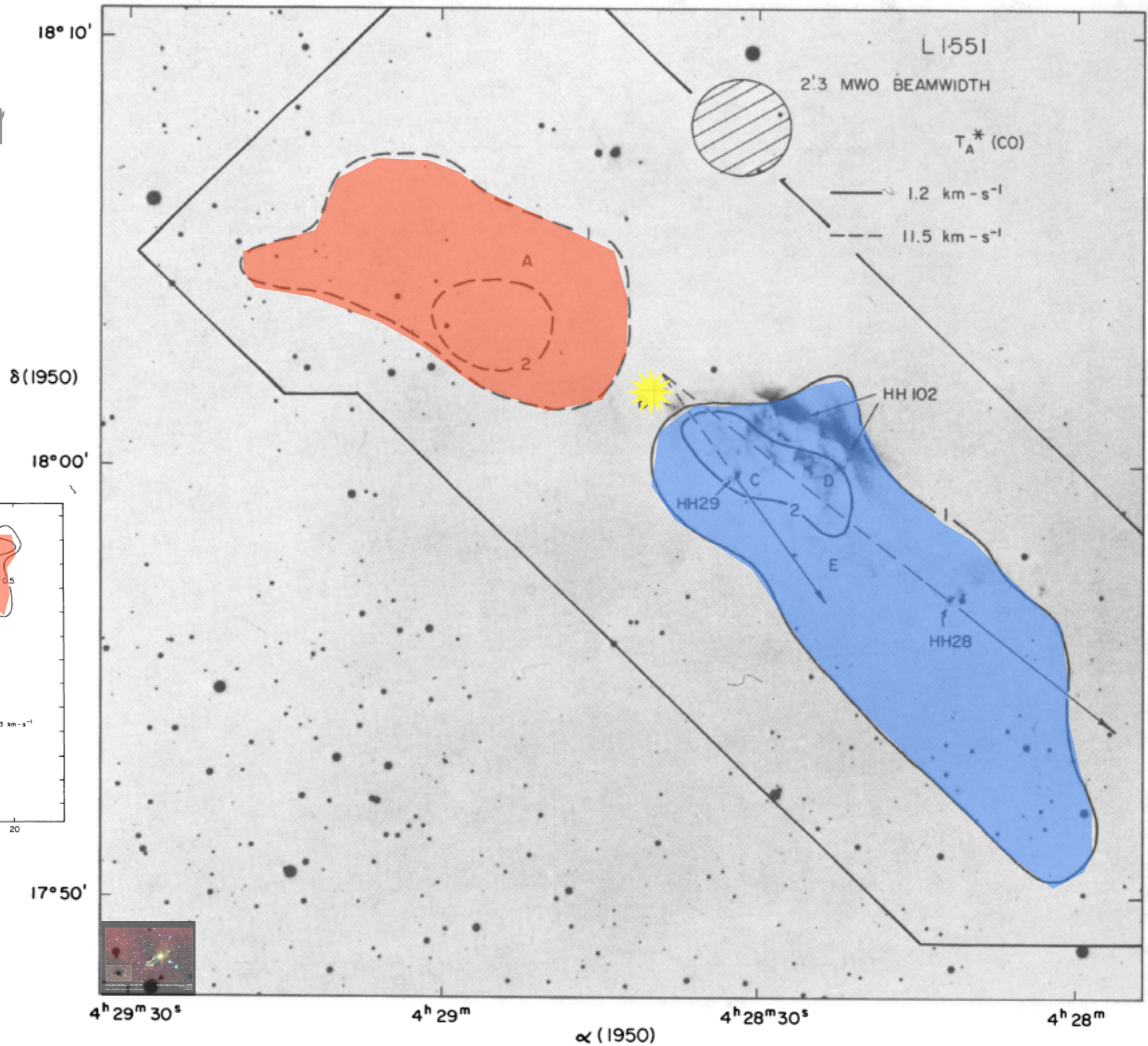
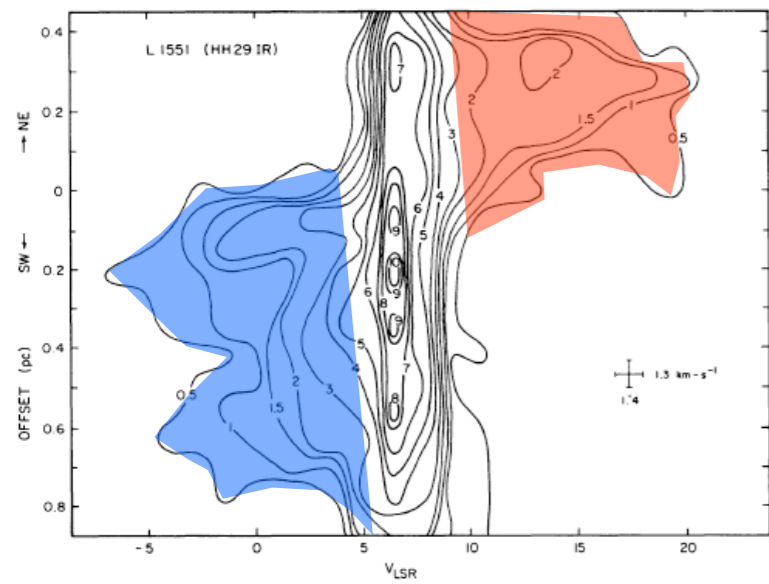
Perseus

3D Viz made with VolView

Outflows

Bipolar & Spher

(!)



Snell, Loren & Plambeck 1980

Outflows

Bipolar & Spheri

(!)

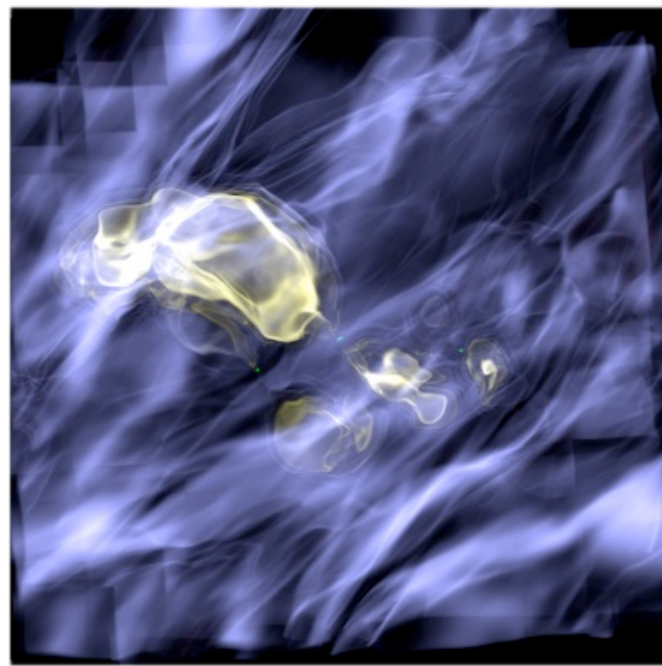
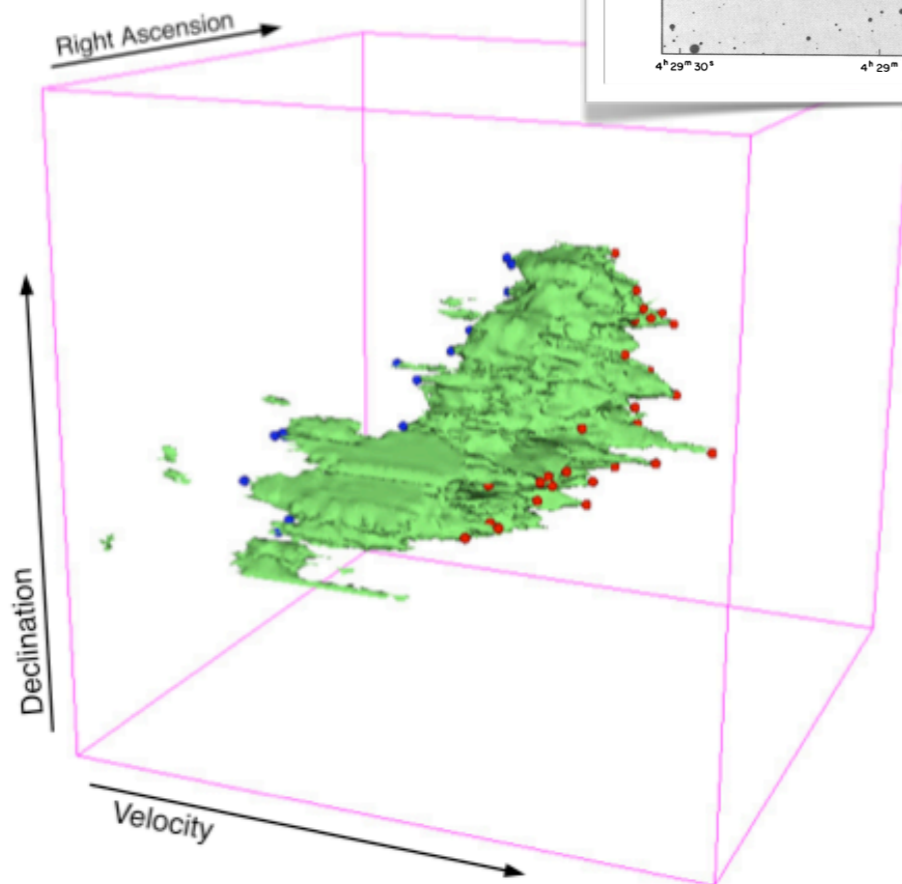
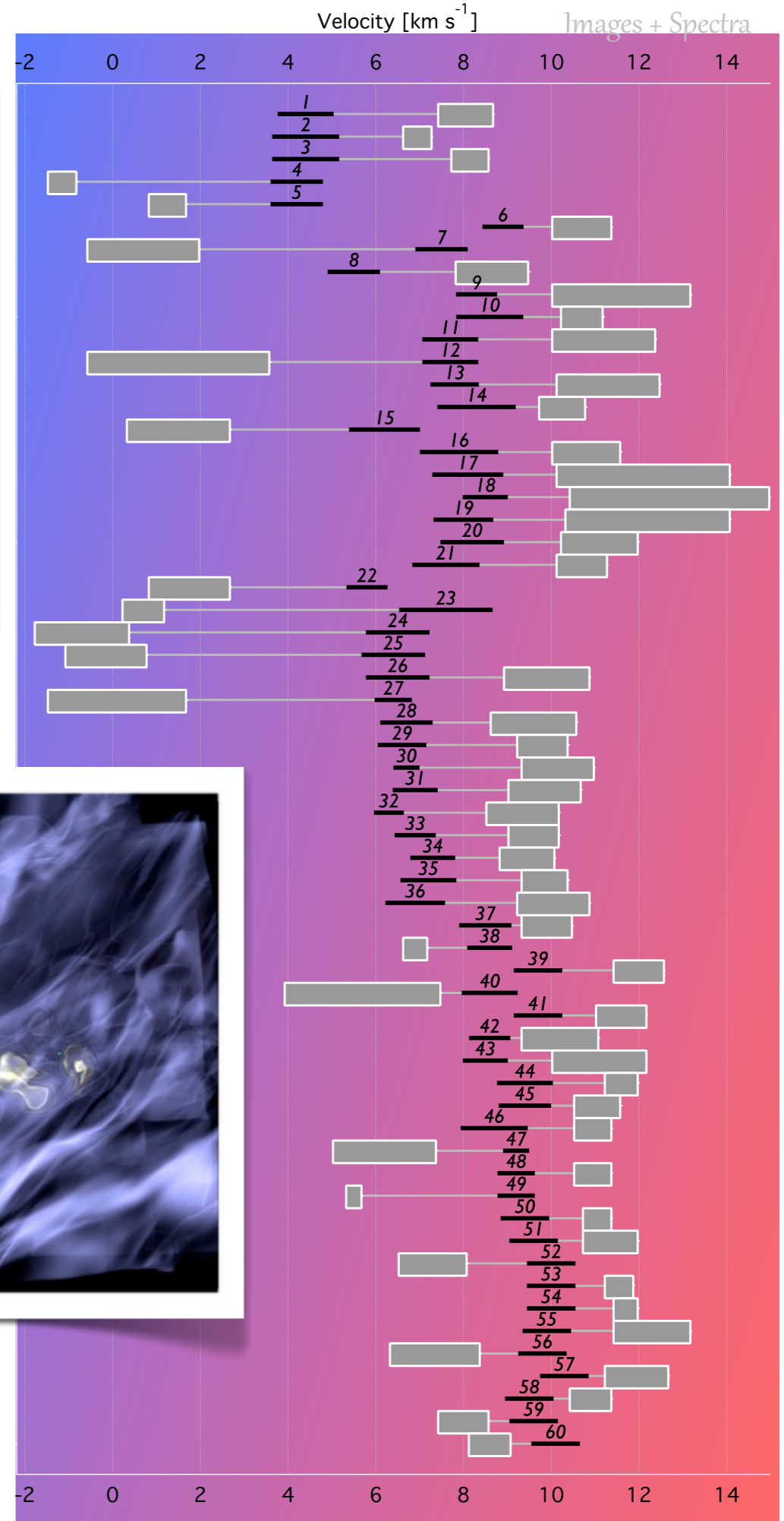
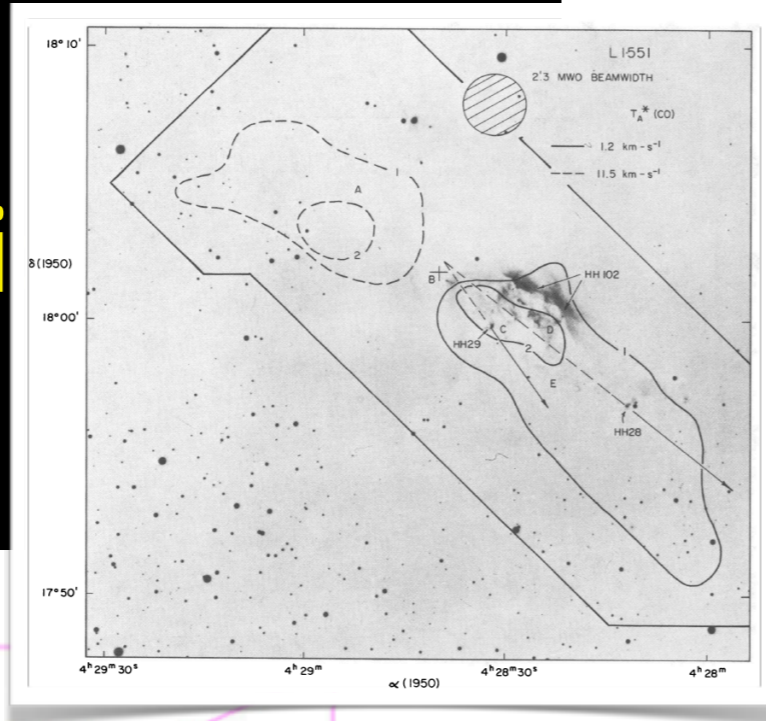


Figure 2. Three-dimensional rendering of the molecular gas in B5 (i.e., Arce VI in Figure 1), using 3D Slicer. The gray (green) isosurface model shows the ¹²CO emission in position–position–velocity space. The small circles show the locations of identified high-velocity points (with the color in the online version representing whether the point is blue- or red-shifted).

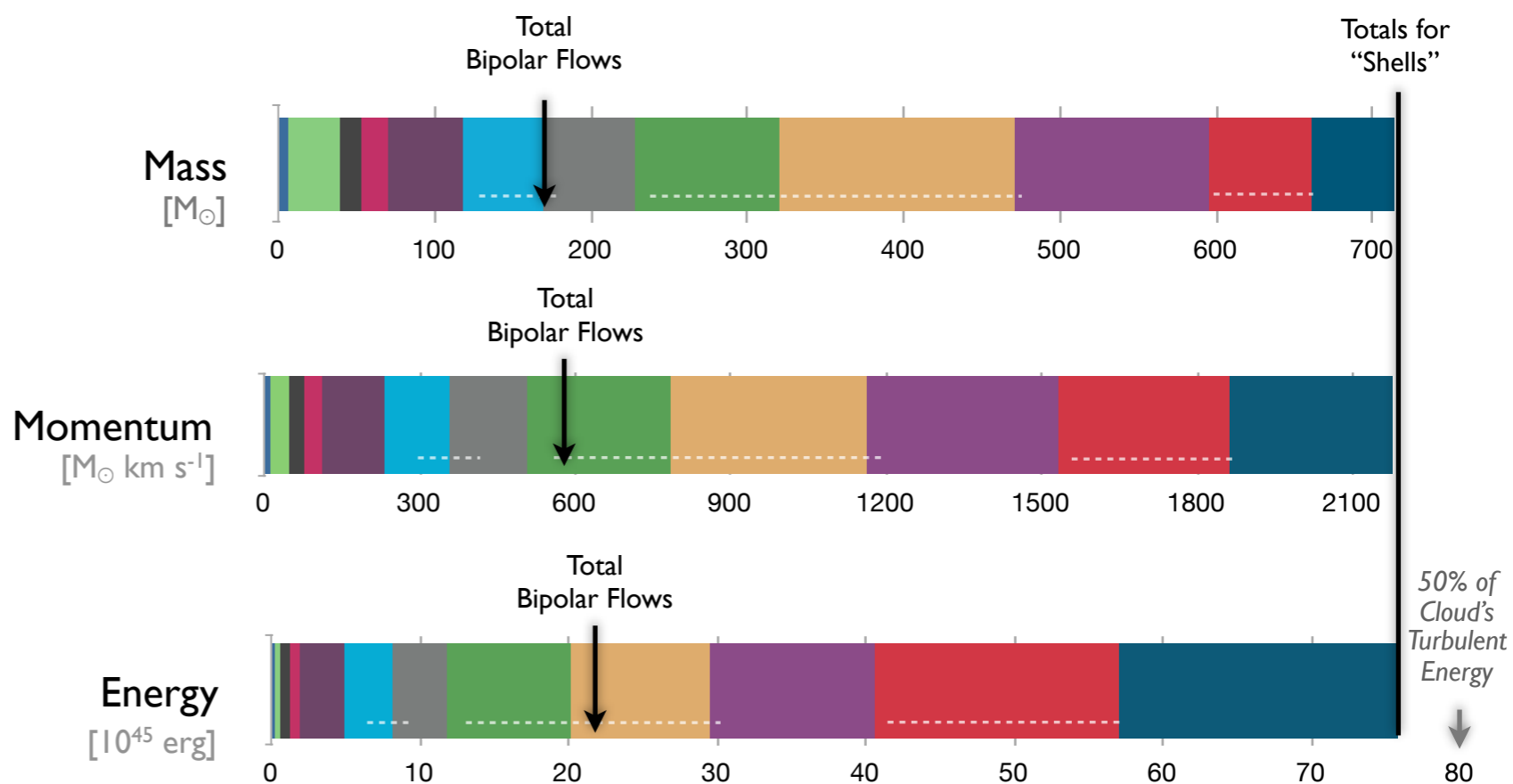
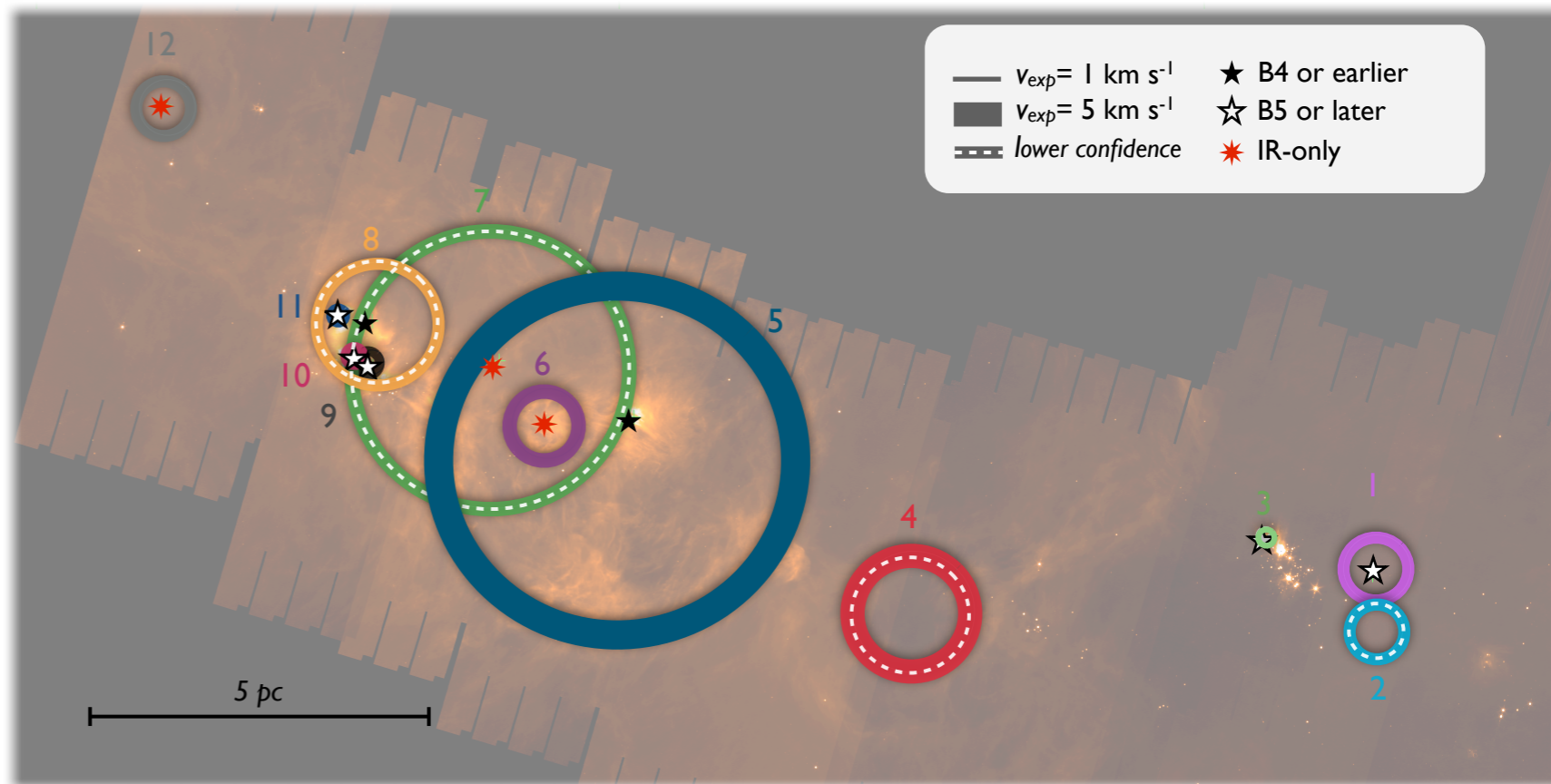
Arce et al. 2010, 2011; simulation from Offner et al. 2011

Outflows

Bipolar & Spherical(!)

News Flash

Spherical shells from young-ish stars may stir molecular clouds (much) MORE than bipolar flows, and B-stars may matter much.



Arce et al. 2011

Theory

Simulation

Images

Spectra

Counting

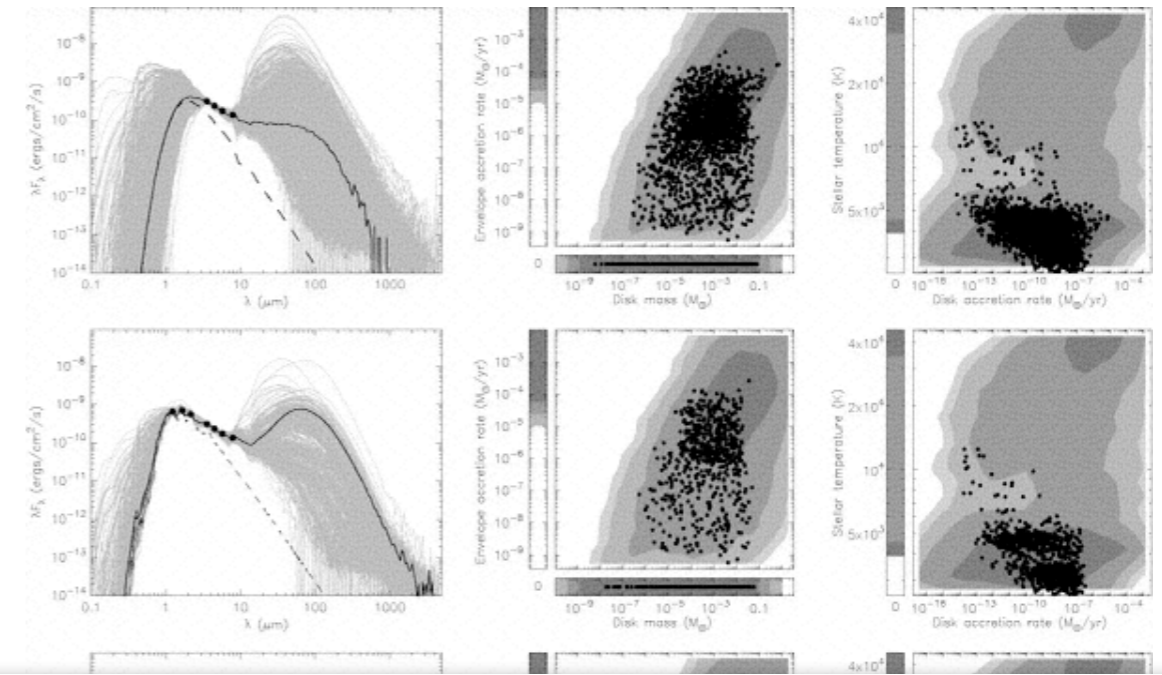
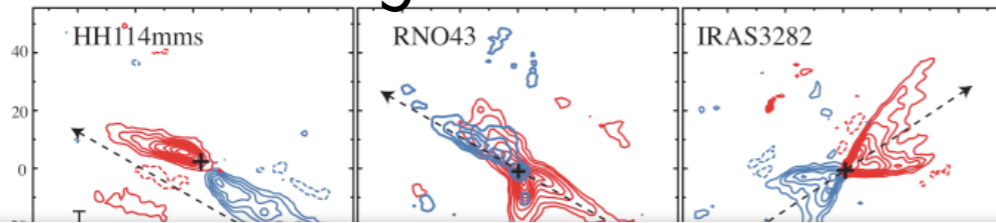
SEDs

Classification

Cataloging

SEDs

Arce & Sargent 2006



How clean an evolutionary sequence can we really measure?
 How similar is one source to another?
 Episodicity of accretion/outflow?

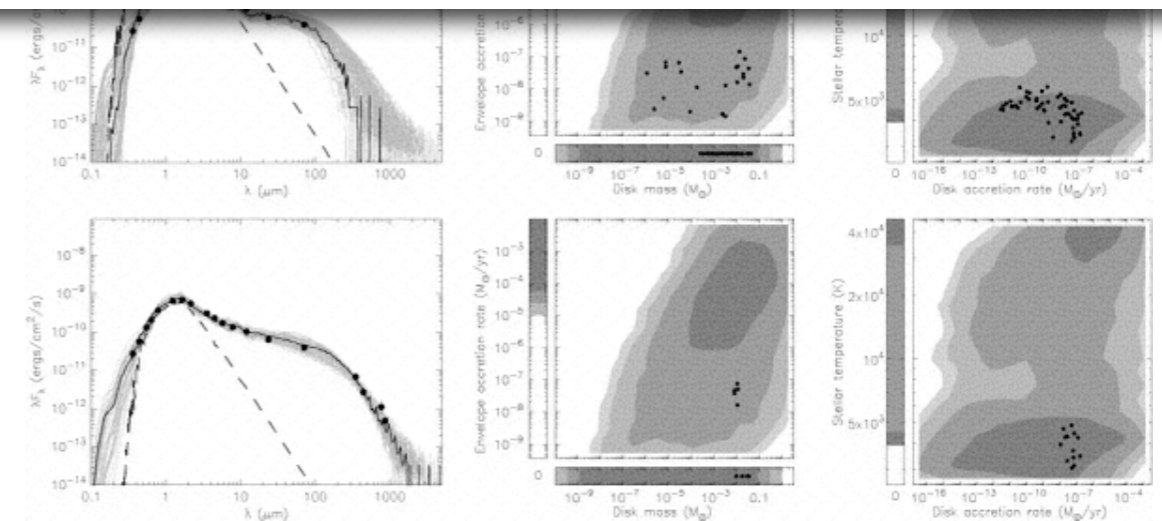
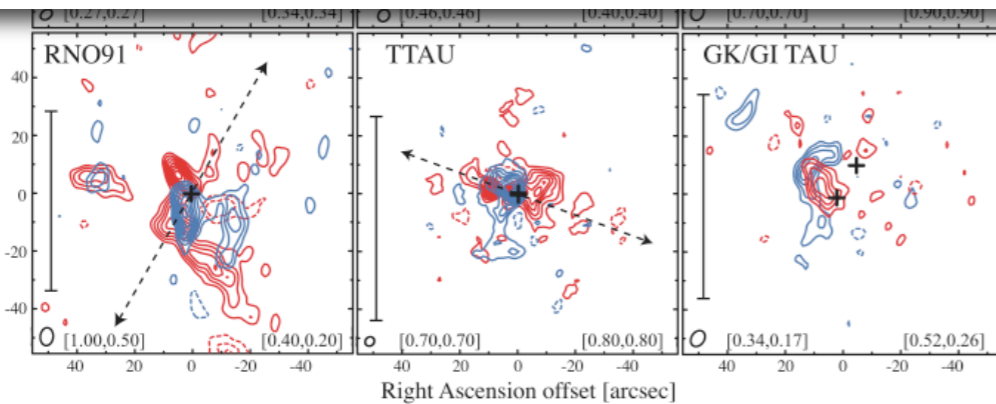


Fig. 1.—Gallery of ^{12}CO (1–0) outflows. Blue (red) contours show the blueshifted (redshifted) emission from the outflow lobes of the sources in our sample, integrated over the velocity ranges given in Table 4. *Top*, Class 0 objects; *middle*, Class I objects; *bottom*, Class II objects. A cross marks the position of the protostar given by the millimeter continuum emission peak. In each map, the synthesized beam is in the lower left corner. A scale equivalent to 10,000 AU at the assumed distance of each source is also given. The dashed line with arrowheads in each panel represents the presumed outflow axis. The values of the first contour and the subsequent contour steps for the blue (red) lobe of each outflow are given inside brackets in units of Jy km s^{-1} , at the lower left (right) corner of each panel.

Classification

First Hydrostatic Core?

Pineda et al. 2011

THE ASTROPHYSICAL JOURNAL, 743:201 (14pp), 2011 December 20

© 2011. The American Astronomical Society. All rights reserved. Printed in the U.S.A.

THE ENIGMATIC CORE L1451-mm: A FIRST HYDROSTATIC

JAIME E. PINEDA^{1,7}, HÉCTOR G. ARCE², SCOTT SCHNEE³, ALYSSA A. GOODMAN⁴,
 THOMAS ROBITAILLE¹, JOEL TANNER², JENS KAUFFMANN^{1,9}, MARIO TAFALLA⁶

¹ Harvard-Smithsonian Center for Astrophysics, 60 Garden Street, Cambridge, MA 02138

² Department of Astronomy, Yale University, P.O. Box 208101, New Haven, CT 06520

³ National Radio Astronomy Observatory, 520 Edgemont Road, Charlottesville, VA 22903

⁴ Observatorio Astronómico Nacional (IGN), Alfonso XII 3, I-48100 Leizor, Spain

⁵ School of Physics and Astronomy, University of Leeds, Leeds LS2 9JT, UK

⁶ Instituto de Astrofísica de Andalucía, CSIC, Apartado 3004, 18014 Granada, Spain

Received 2011 March 29; accepted 2011 September 6; published 2011 December 20

ABSTRACT

We present the detection of a dust continuum source at 3 mm (CARMA) and ¹²CO (2–1) emission (SMA) toward the L1451-mm dense core. The detection of a continuum source and an outflow where no point source at mid-infrared wavelengths is detected. A dense core bolometric luminosity of 0.05 L_⊙ is obtained. By modeling the continuum emission and the continuum interferometric visibilities simultaneously, we confirm that the data can be explained by a stellar object (YSO) and a disk, or by a dense core with a central first hydrostatic core (FHSC). We are not able to decide between these two models, which produce similar fits. The detection of redshifted and blueshifted emission suggesting the presence of a slow outflow is not what is usually found toward YSOs but in agreement with prediction from models for a FHSC. The best candidate, so far, for an FHSC, an object that has been identified in the literature. Whatever the true nature of the central object in L1451-mm, this core presents characteristics of the earliest phases of low-mass star formation.

Key words: ISM: clouds – ISM: individual objects (L1451, Perseus) – Infrared: stars – low-mass

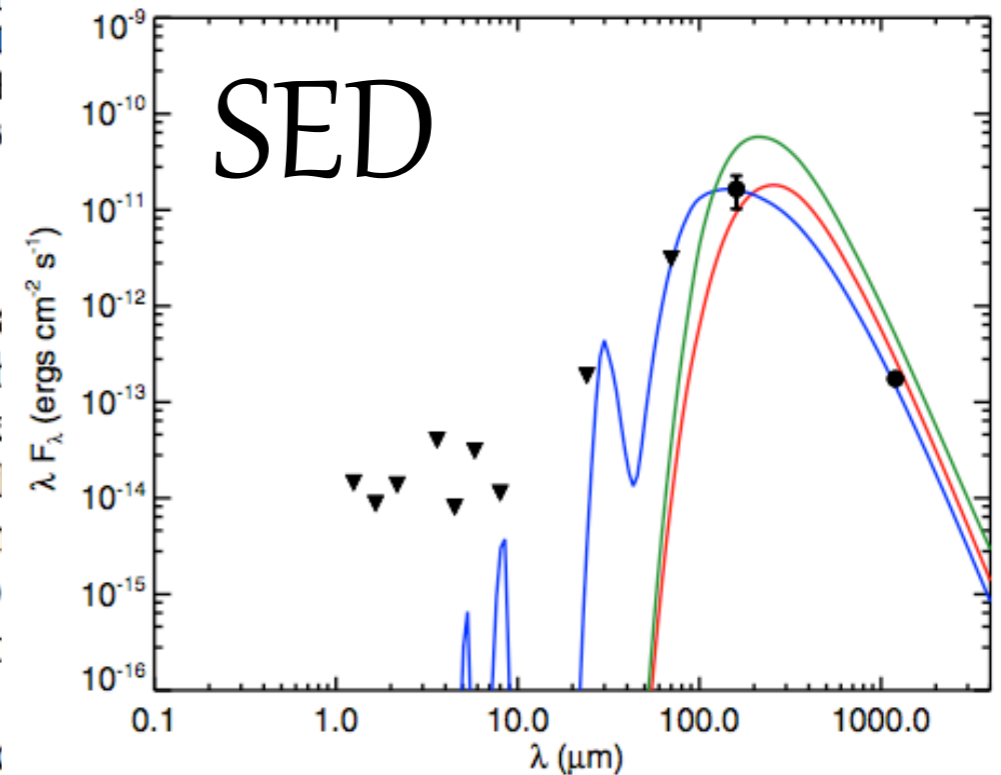
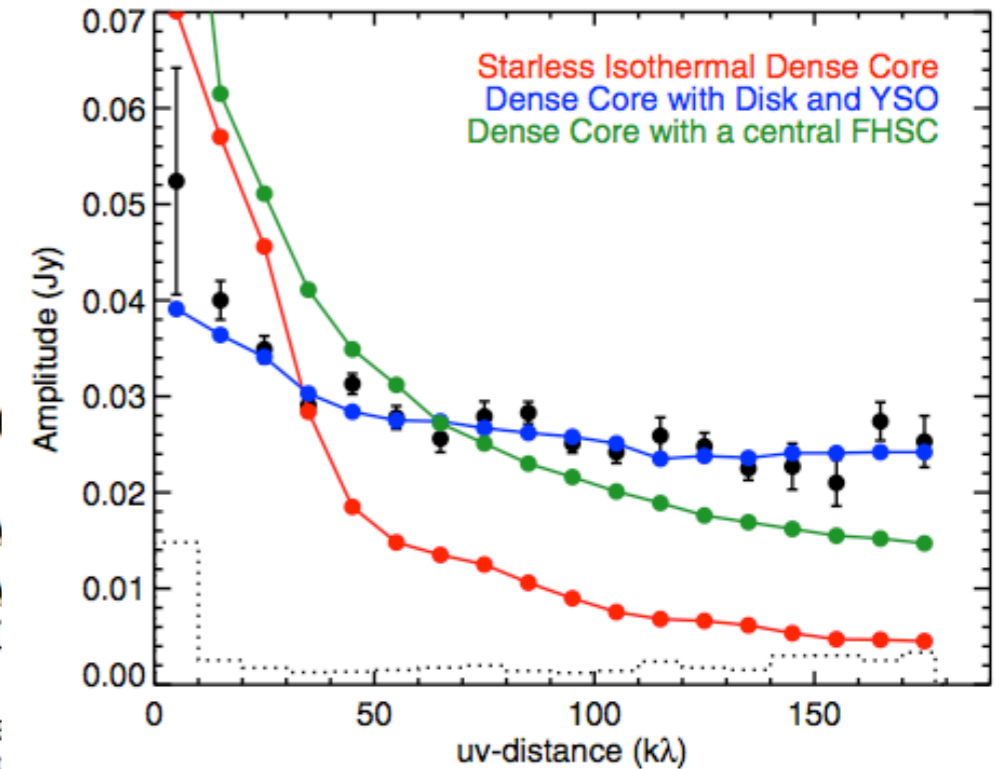


Figure 9. Summary of best fit of the broadband SED and dust continuum visibilities for three different models: starless isothermal dense core in red, dense core with a YSO and disk at the center in blue, and dense core with a central FHSC in green. The data are shown in black. The top panel shows the visibilities in filled circles. The bottom panel shows the broadband SED for L1451-mm, where the upper limits are shown by triangles, measurements are shown by filled black circles, and the best model fits are shown by the solid curves.

SEDs

A new
Bayesian
“story” you
should
remember

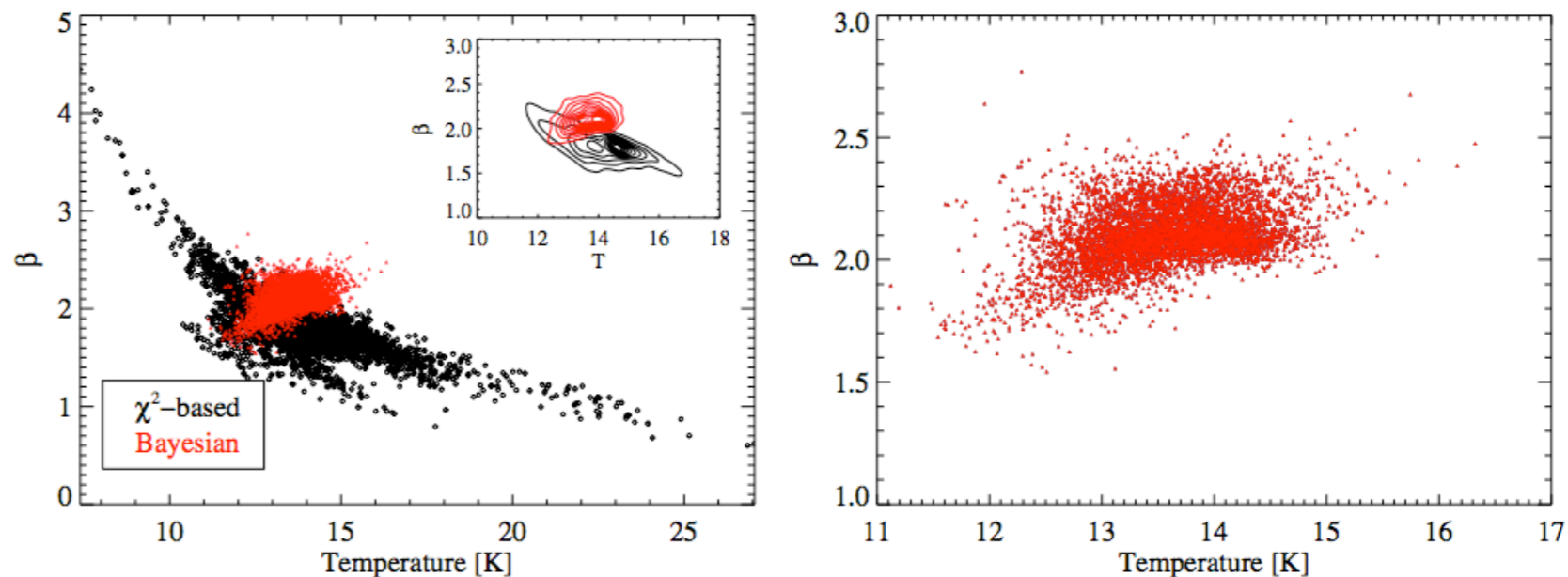


Figure 6. Left panel shows the distribution of β and T for CB244 from minimizing χ^2 (black open circles) and the random draw from the posterior distribution under our hierarchical Bayesian model (red triangles). The inset provides a close-up of the density of the distribution, while the right panel shows a close-up of the hierarchical Bayesian values. As expected, the χ^2 -based estimates display an anti-correlation. However, the Bayesian estimates show a weak positive correlation, and there is a large range in β at fixed T .
(A color version of this figure is available in the online journal.)

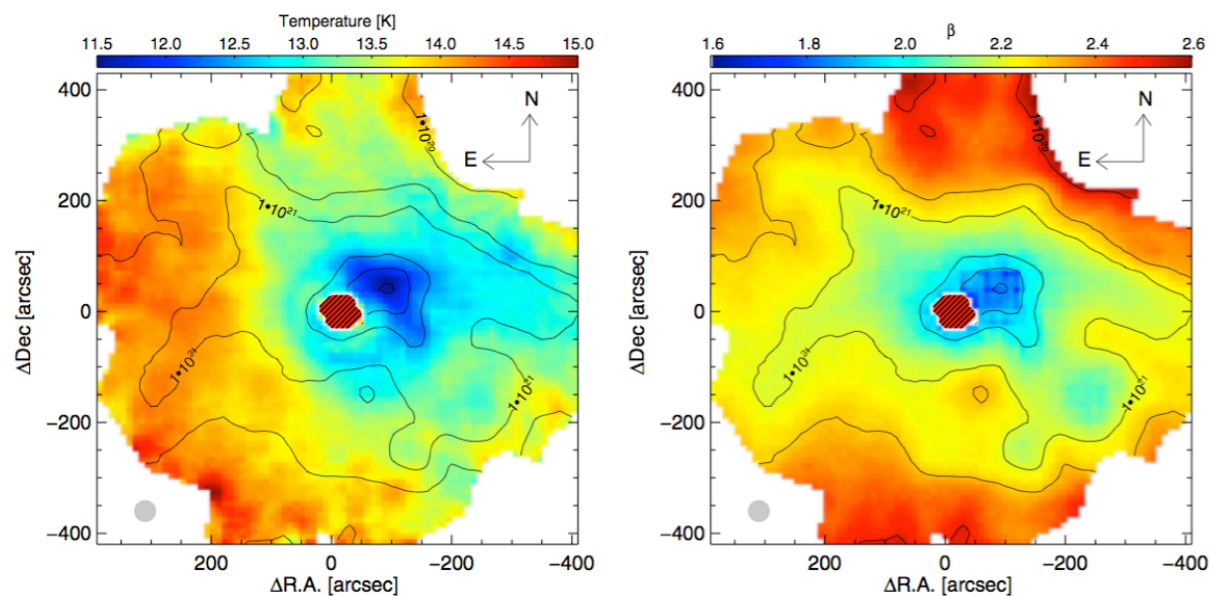


Figure 8. Temperature (left) and β (right) map for CB244 derived from the Bayesian estimates. The red hashed region in the center of the images corresponds to the protostar, which we exclude from our analysis, and the gray circle in the lower left corner illustrates the size of the SPIRE $500\ \mu\text{m}$ beam. Overplotted are contours of constant column density, corresponding to $N(\text{H}) = 10^{20}, 5 \times 10^{20}, 10^{21}, 5 \times 10^{21}, 10^{22}$, and $2 \times 10^{22}\ \text{cm}^{-2}$. The coolest and most dense region corresponds to the prestellar core, with the temperature decreasing toward its center. The β -map traces the column density map very well, with the values of β decreasing toward the central, more dense regions.

(A color version of this figure is available in the online journal.)

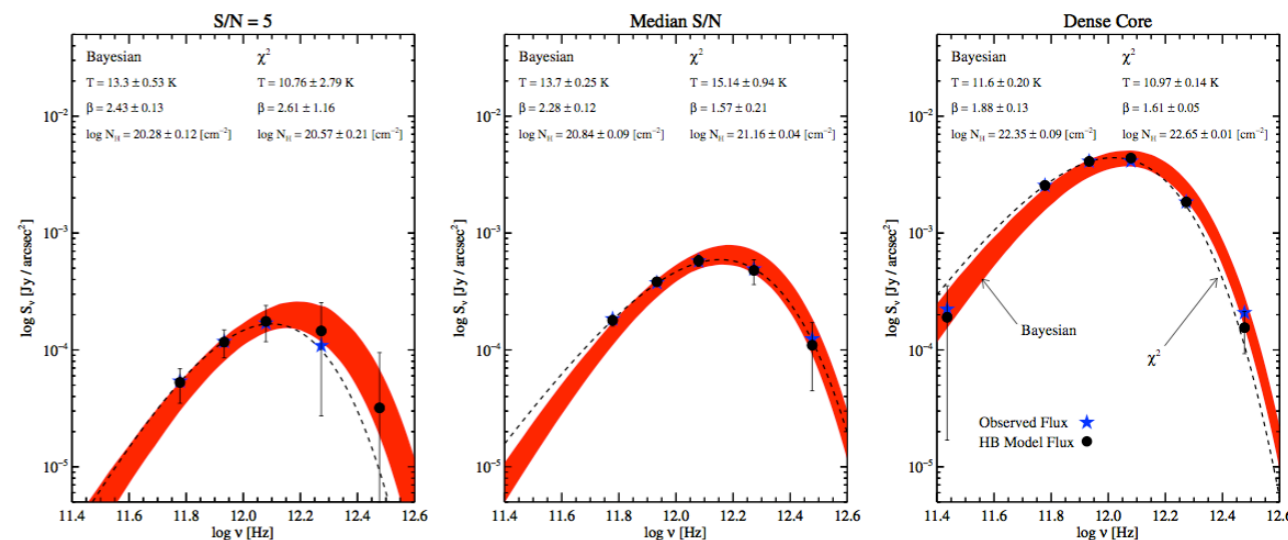


Figure 7. Measured fluxes (blue stars) for the pixel with the highest estimated column density in the prestellar core (right), a pixel with average *Herschel* S/N similar to the median value (center), and the pixel with average *Herschel* S/N = 5 (left), which defines the lower limit of our S/N cut for the χ^2 estimates. The $100\ \mu\text{m}$ flux measurement is missing from the left panel because its value is negative. The best-fit graybody SEDs derived from the χ^2 estimates are shown with a dashed black line, while the red regions contain 95% of the posterior probability for the graybody SEDs derived from our hierarchical Bayesian method. The measured fluxes are compared with the values that are predicted from our Bayesian model (black circles), with the error bars containing 95% of the posterior probability on the measured SED. The fluxes and their error bars predicted from our Bayesian model differ from the model graybody SEDs in that they also include the effects of the calibration error and noise, and thus it is the green circles that should be compared with the measured data and not the red region. The actual measured values of the flux fall within the range expected from our Bayesian model, and therefore our model is consistent with the measured data.

(A color version of this figure is available in the online journal.)

Kelly, Shetty, et al. 2012

Spectra Bayesian analysis of Zeeman measurements of \mathbf{B} in ISM

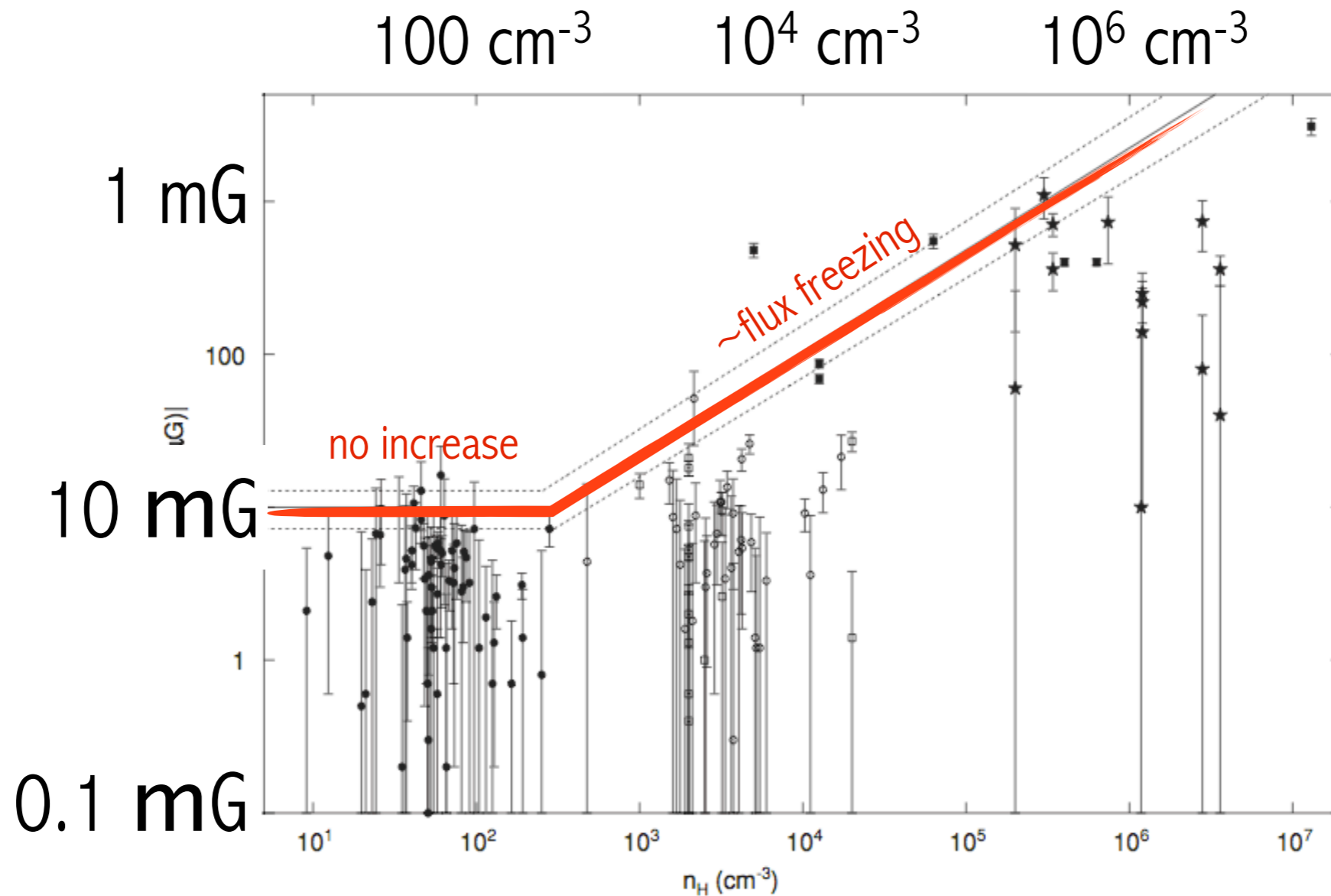


Figure 1. Set of diffuse cloud and molecular cloud Zeeman measurements of the magnitude of the line-of-sight component B_z of the magnetic vector \mathbf{B} and their 1σ uncertainties, plotted against $n(\text{H}) = n(\text{HI})$ or $2n(\text{H}_2)$ for HI and molecular clouds, respectively. Different symbols denote the nature of the cloud and source of the measurement: HI diffuse clouds, filled circles (Heiles & Troland 2004); dark clouds, open circles (Troland & Crutcher 2008); dark clouds, open squares (Crutcher et al. 1999), molecular clouds, filled squares (Crutcher et al. 1999); and molecular clouds, stars (Falgarone et al. 2008). Note that Zeeman measurements give the direction of the line-of-sight component as well as the magnitude. By convention, positive B_z denote fields pointing away from the observer and vice versa. Only the magnitudes $|B_z|$ are plotted. The solid line segments show the most probable model from the comprehensive analysis, Section 6. Also shown (plotted as dotted line segments) are the ranges given by acceptable alternative model parameters to indicate on the B_z plane the uncertainty in the model.

Crutcher et al. 2010

Theory

Simulation

Images

Spectra

Counting

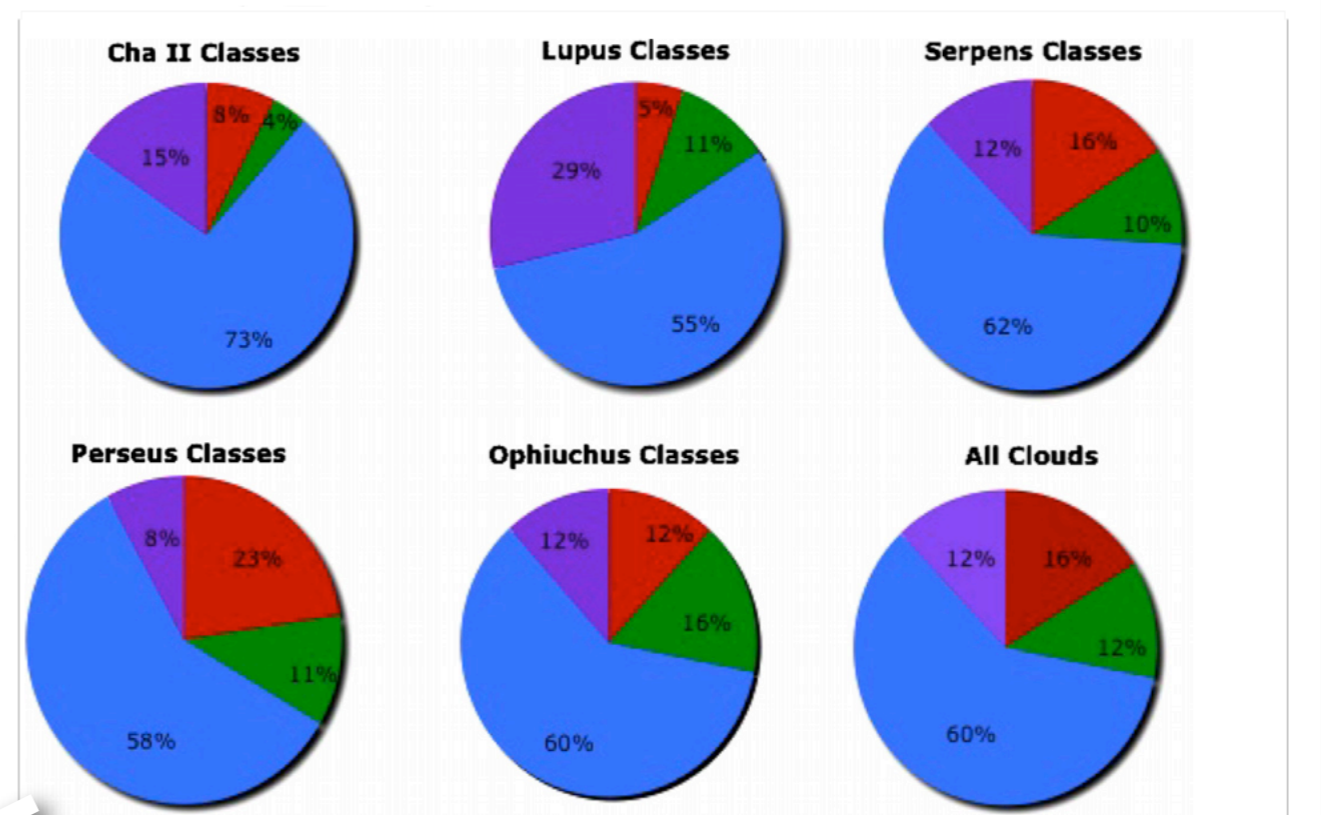
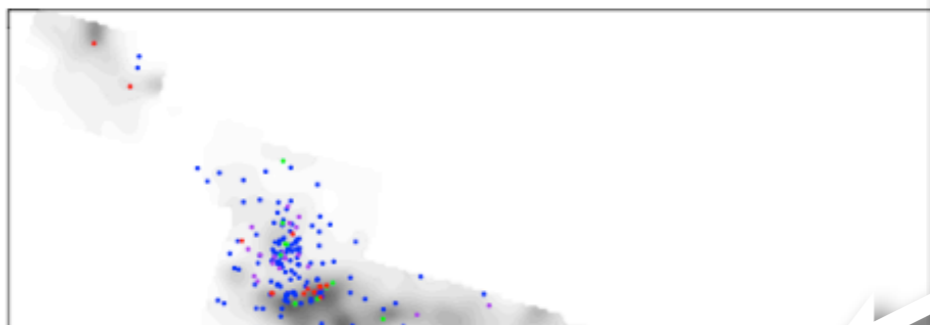
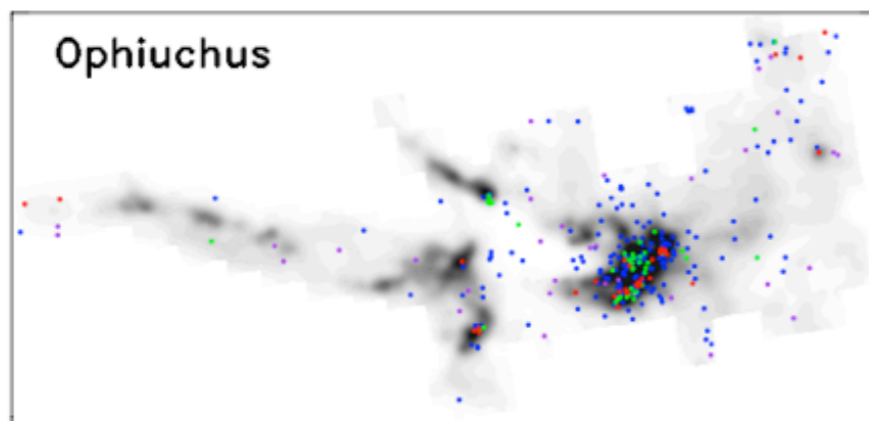
SEDs

Classification

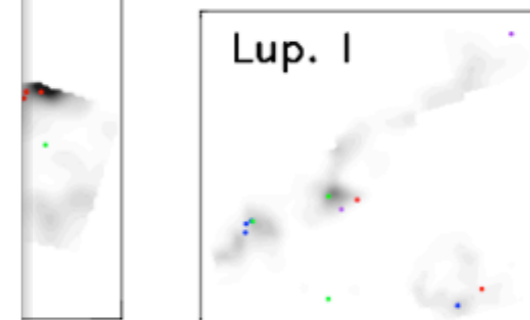
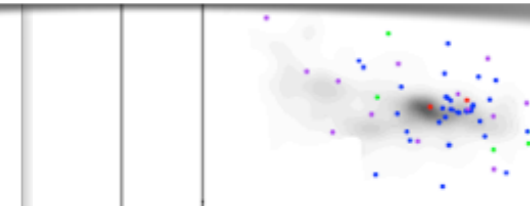
Cataloging



Classification Cataloging Counting



The derived lifetime for the Class I phase is 0.54 Myr, considerably longer than some estimates. Similarly, the lifetime for the Class 0 SED class, 0.16 Myr, with the notable exception of the Ophiuchus cloud, is longer than early estimates. If photometry is corrected for estimated extinction before calculating class indicators, the lifetimes drop to 0.44 Myr for Class I and to 0.10 for Class 0. These lifetimes assume a continuous flow through the Class II phase and should be considered median lifetimes or half-lives. Star formation is highly concentrated to regions of high extinction, and the youngest objects are very strongly associated with dense cores. The great majority (90%) of young stars lie within loose clusters with at least 35 members and a stellar density of $1 M_{\odot} \text{ pc}^{-3}$.



the bar. All YSOs are plotted with the following

Evans et al. 2009

cf. Elias 1978

Larson's "Suggestions"



1981MNRAS.194..809L

Mon. Not. R. astr. Soc. (1981) **194**, 809–826

Turbulence and star formation in molecular clouds

Richard B. Larson *Yale University Observatory, Box 6666, New Haven, Connecticut 06511, USA*

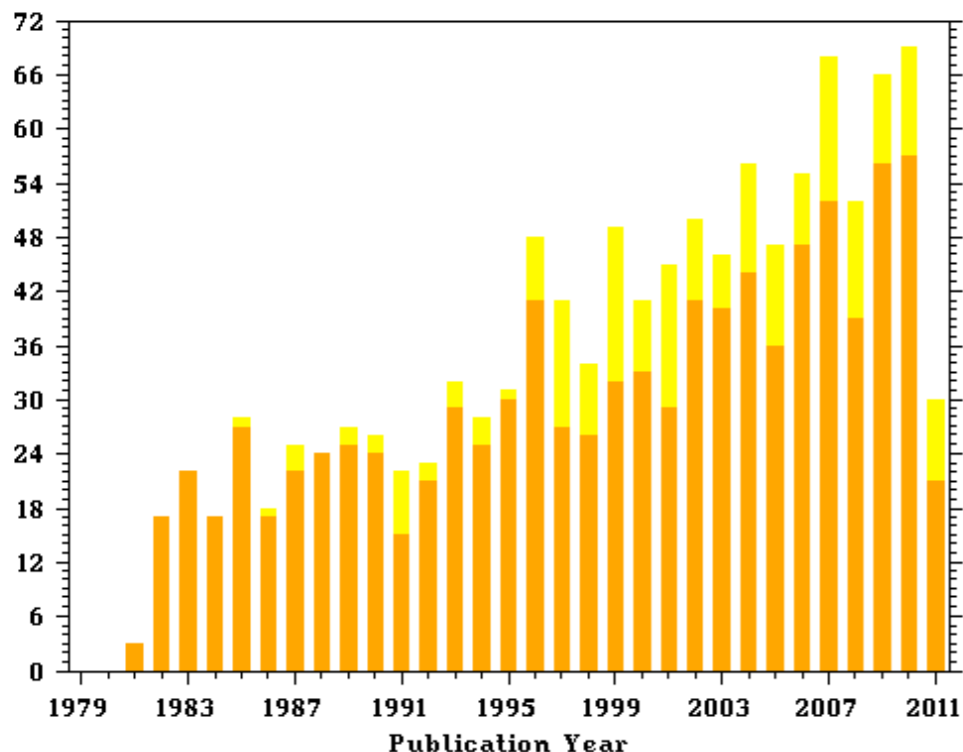
Received 1980 July 7; in original form 1980 May 7

Summary. Data for many molecular clouds and condensations show that the internal velocity dispersion of each region is well correlated with its size and mass, and these correlations are approximately of power-law form. The dependence of velocity dispersion on region size is similar to the Kolmogoroff law for subsonic turbulence, suggesting that the observed motions are all part of a common hierarchy of interstellar turbulent motions. The regions studied are mostly gravitationally bound and in approximate virial equilibrium. However, they cannot have formed by simple gravitational collapse, and it appears likely that molecular clouds and their substructures have been created at least partly by processes of supersonic hydrodynamics. The hierarchy of subcondensations may terminate with objects so small that their internal motions are no longer supersonic; this predicts a minimum protostellar mass of the order of a few tenths of a solar mass. Massive 'protostellar' clumps always have supersonic internal motions and will therefore develop complex internal structures, probably leading to the formation of many pre-stellar condensation nuclei that grow by accretion to produce the final stellar mass spectrum. Molecular clouds must be transient structures, and are probably dispersed after not much more than 10^7 yr.

1 Introduction

There is much evidence that stars form in the interiors of dense, gravitationally bound molecular clouds, but little is yet known about the detailed internal structure and dynamics of such clouds, or about the processes by which stars form in them. This lack of direct information has allowed theorists considerable scope for calculating idealized models for the collapse and fragmentation of gas clouds, starting with simple assumed initial conditions (see the reviews by Larson 1977a; Woodward 1978; Bodenheimer & Black 1978). Much of this work has been motivated by the 'gravitational instability' picture of star formation elaborated by Jeans (1929), Hoyle (1953) and Hunter (1967), whereby diffuse clouds that are initially nearly uniform collapse and fragment into a hierarchy of successively smaller condensations as the density rises and the Jeans mass decreases.

Citations/Publication Year for 1981MNRAS.194..809L



~Virial Equilibrium: Gravity Balanced by “Turbulent” Support

The dashed line in this figure is not fitted to the points, but represents the relation

$$\frac{2GM}{\sigma^2 L} = 0.92 L (\text{pc})^{0.14} \quad (4)$$

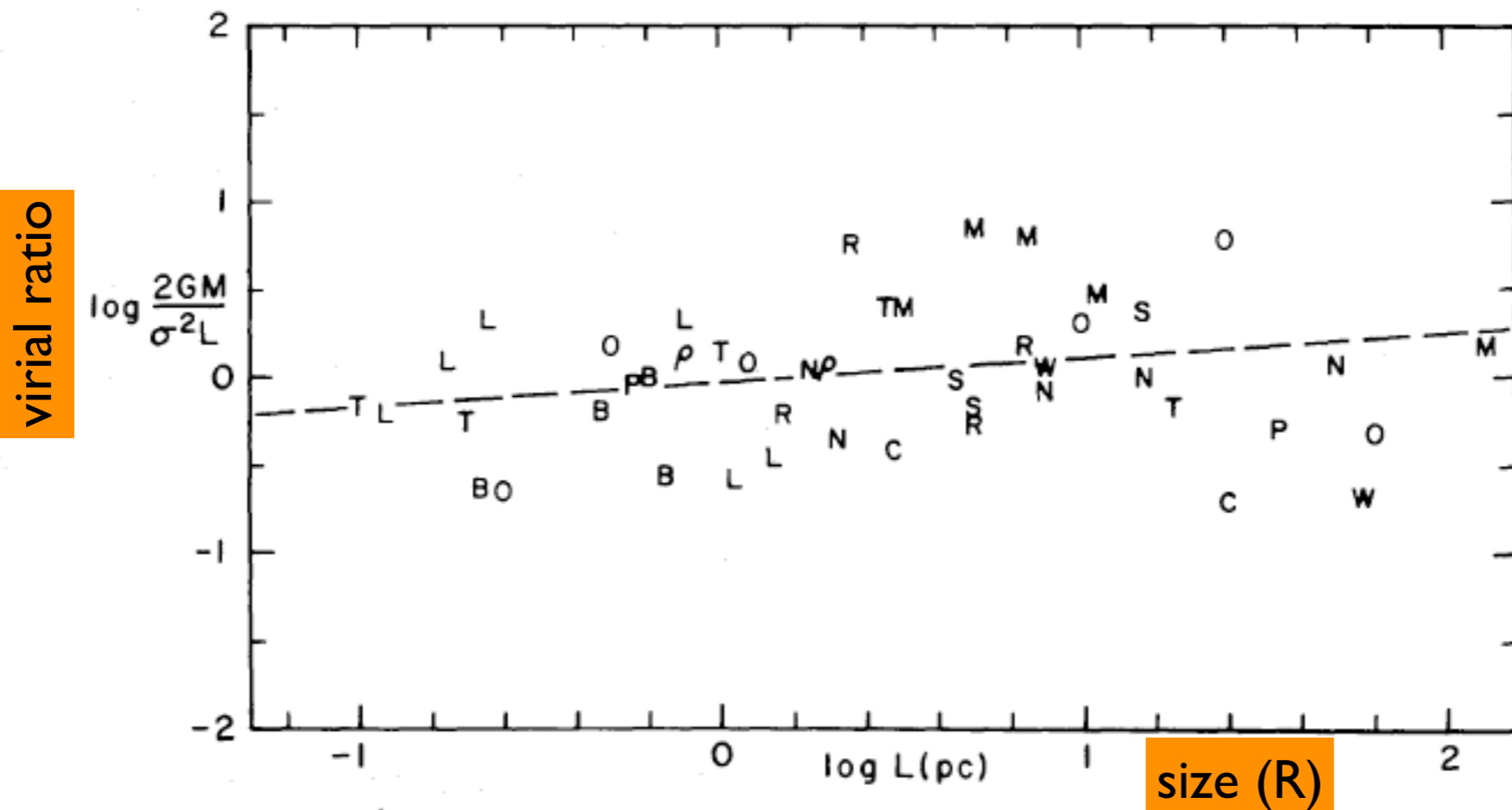


Figure 4. The virial ratio $2GM/\sigma^2 L$ plotted versus region size L for the same regions shown in Figs 1 and 2. The dashed line represents equation (4), and is derived from equations (1) and (2).

for exact virial equilibrium, $2GM/R^2 \sigma^2 = 1$, and points above would be on horizontal line

“Density - size” $n \sim R^{-1.1}$

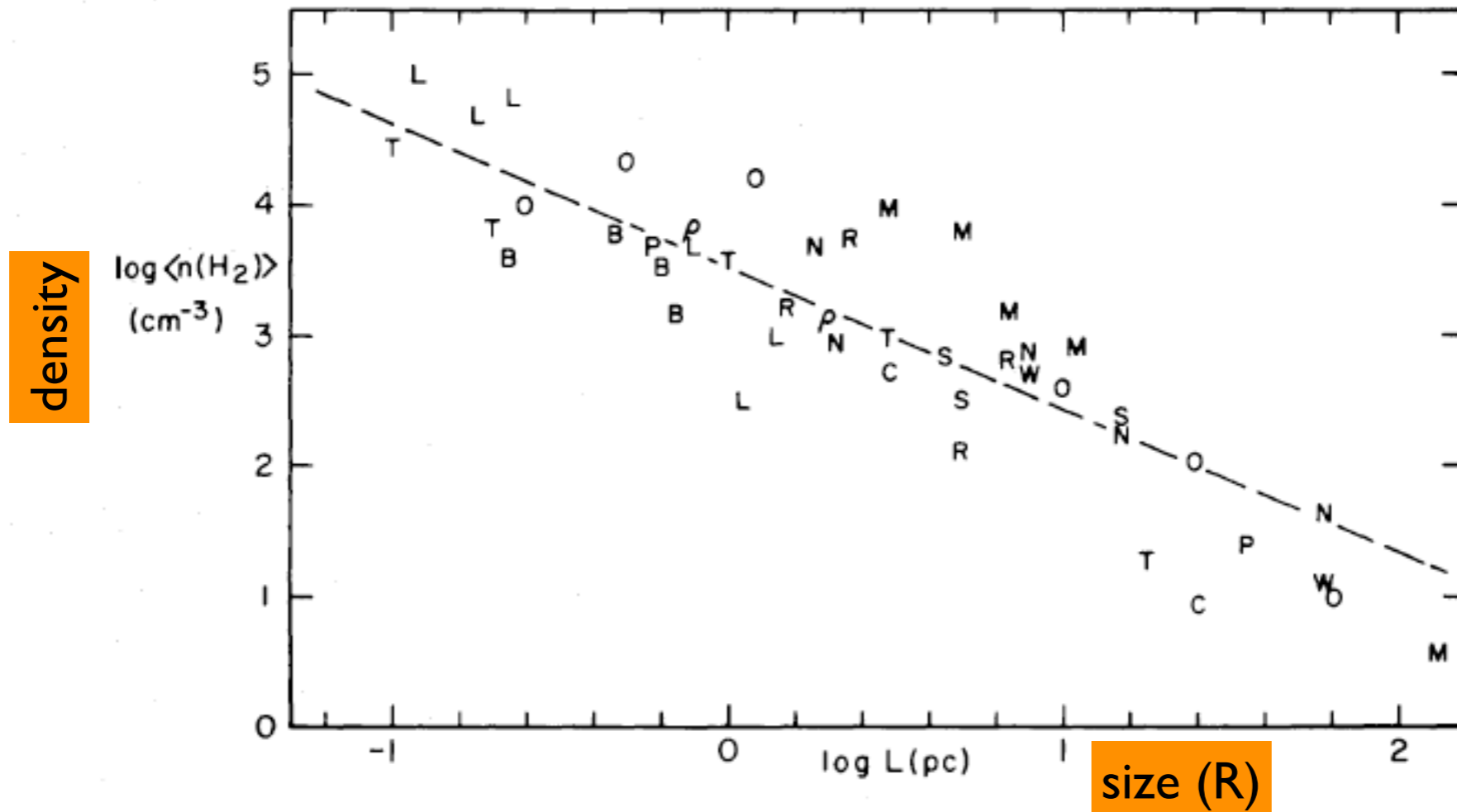


Figure 5. The average density, defined as the density of a sphere of mass M and diameter L , of all the regions shown in Figs 1 and 3 plotted versus region size L . The dashed line represents equation (5), and is derived from equations (1) and (2).

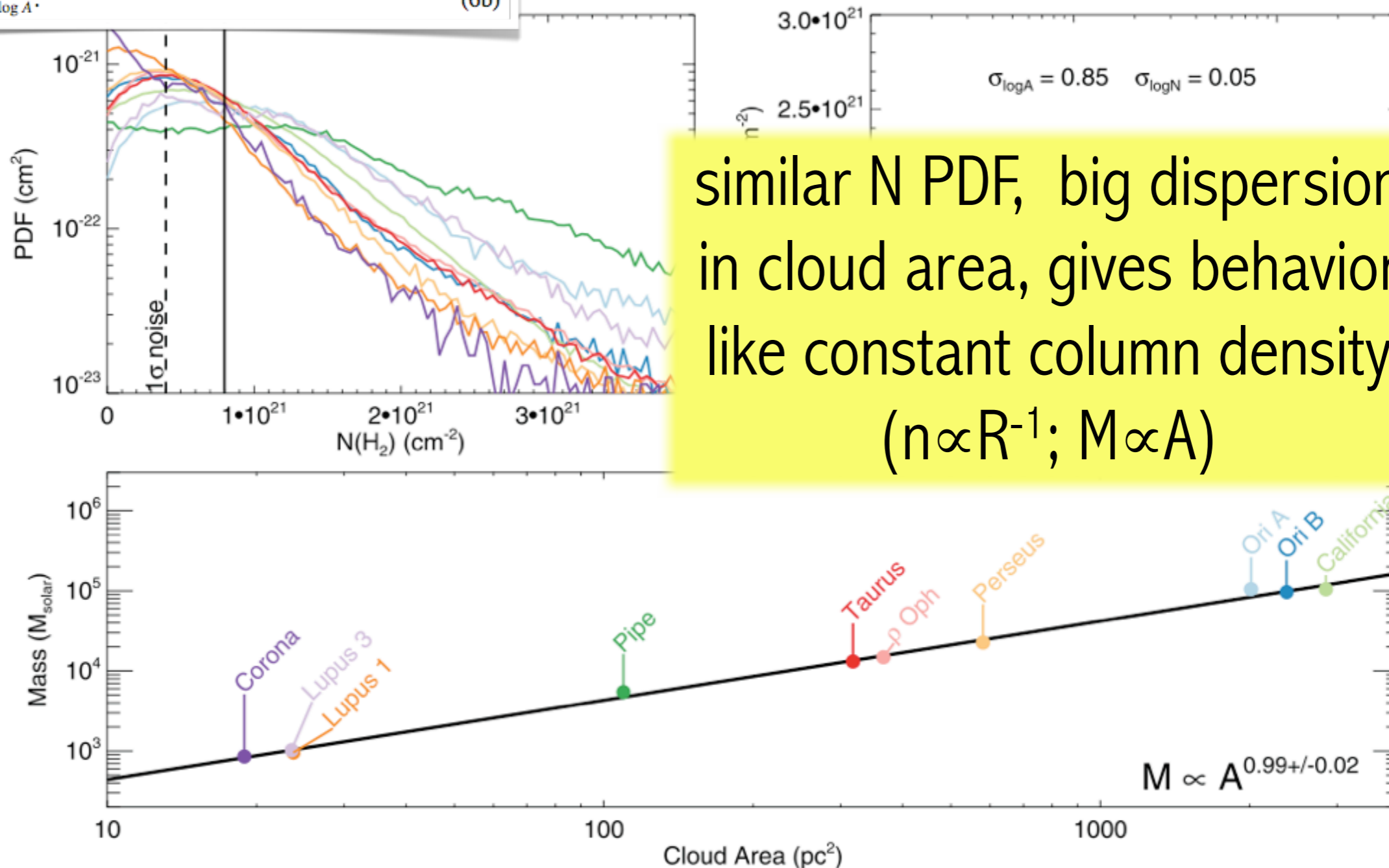
For $n \sim R^{-1}$, and $s \sim R^{0.5}$, and $2GM/R^2s^2 = 1$ (virial equilibrium)
 any one relation follows automatically from the other two

So, roughly speaking, Larson's "Suggestions" show that a *turbulent-like nature for the line width-size relation, plus virial equilibrium, gives the observed density-size relation.*

Thus, the precision at which L3 is recovered will be high when the dispersion of PDF means is small compared to the dispersion in areas. In summary, the conditions sufficient for a sample of mass and area measurements to follow L3 with low scatter are

$$\langle N \rangle \propto A \quad (6a)$$

$$\sigma_{\log(N)}^2 \ll q \sigma_{\log A}^2 \quad (6b)$$



similar N PDF, big dispersion in cloud area, gives behavior like constant column density ($n \propto R^{-1}$; $M \propto A$)

Figure 4. The connection between the column density PDF and mass–area relationship for the data presented in LAL10. Left: the column density PDF for each cloud. Right: the mean column density of pixels with extinctions higher than the threshold defined by the solid line on the left-hand plot, as a function of the cloud area. Bottom: the mass–area relationship.

Beaumont et al. 2012; cf. Lombardi, Alves & Lada 2010

Is there a transition to a “thermal” regime? Does gravity matter more there?

THE ASTROPHYSICAL JOURNAL, 504:223–246, 1998 September 1
© 1998. The American Astronomical Society. All rights reserved. Printed in U.S.A.

COHERENCE IN DENSE CORES. II. THE TRANSITION TO COHERENCE

ALYSSA A. GOODMAN¹

Harvard University Department of Astronomy, Cambridge, MA 02138; agoodman@cfa.harvard.edu

JOSEPH A. BARRANCO

Astronomy Department, University of California, Berkeley, Berkeley, CA 94720; barranco@ucbast.berkeley.edu

DAVID J. WILNER

Harvard-Smithsonian Center for Astrophysics, 60 Garden Street, Cambridge, MA 02138; dwilner@cfa.harvard.edu

AND

MARK H. HEYER

Five College Radio Astronomy Observatory, University of Massachusetts, Amherst, MA 01003; heyer@fcrao1.phast.umass.edu

Received 1997 June 17; accepted 1998 February 5

ABSTRACT

After studying how line width depends on spatial scale in low-mass star-forming regions, we propose that “dense cores” (Myers & Benson 1983) represent an inner scale of a self-similar process that characterizes larger scale molecular clouds.

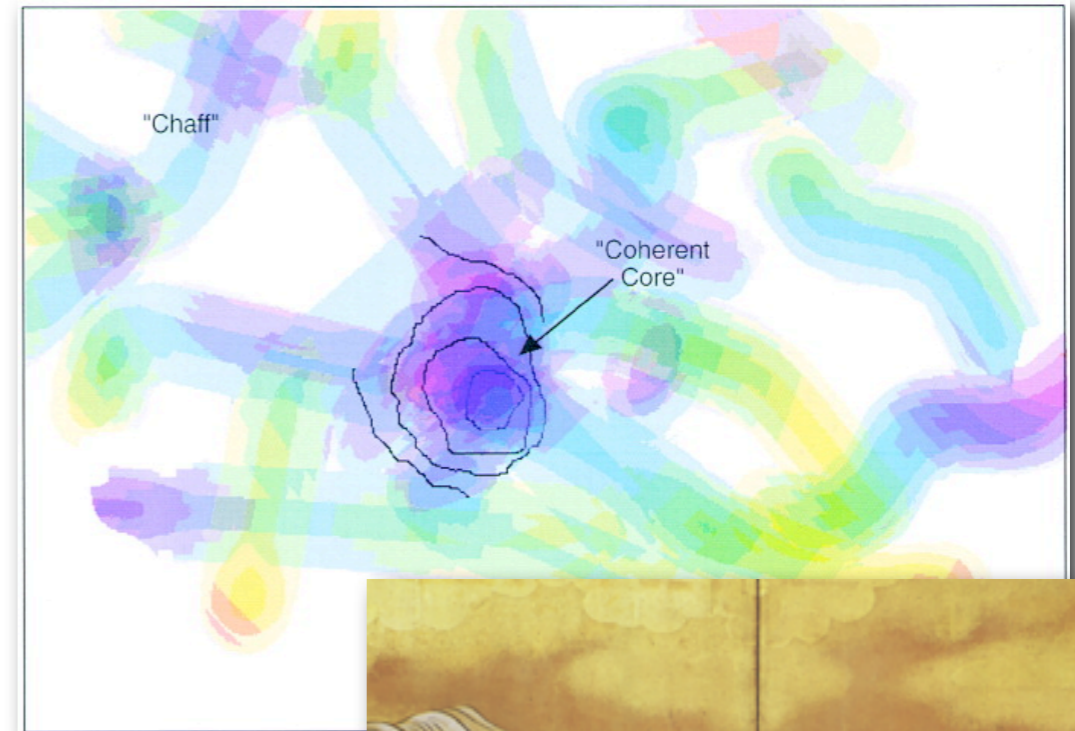
In the process of coming to this conclusion, we define four distinct types of line width–size relation ($\Delta v \propto R^a$), which have power-law slopes a_1 , a_2 , a_3 , and a_4 , as follows: Type 1—multitracer, multicloud intercomparison; Type 2—single-tracer, multicloud intercomparison; Type 3—multitracer study of a single cloud; and Type 4—single-tracer study of a single cloud. Type 1 studies (of which Larson 1981 is the seminal example) are compendia of Type 3 studies which illustrate the range of variation in the line width–size relation from one region to another.

Using new measurements of the OH and C¹⁸O emission emanating from the environs of several of the dense cores studied in NH₃ by Barranco & Goodman (1998; Paper I), we show that line width increases with size outside the cores with $a_4 \sim 0.2$. On scales larger than those traced by C¹⁸O or OH, ¹²CO and ¹³CO observations indicate that a_4 increases to ~ 0.5 (Heyer & Schloerb 1997). By contrast, within the half-power contour of the NH₃ emission from the cores, line width is virtually constant, with $a_4 \sim 0$. We interpret the correlation between increasing density and decreasing Type 4 power-law slope as a “transition to coherence.” Our data indicate that the radius R_{coh} at which the gas becomes coherent (i.e., $a_4 \rightarrow 0$) is of order 0.1 pc in regions forming primarily low-mass stars. The value of the *nonthermal* line width at which “coherence” is established is always less than but still of order of the thermal line width of H₂. Thus coherent cores are similar to, but not exactly the same as, isothermal balls of gas.

Two other results bolster our proposal that a transition to coherence takes place at ~ 0.1 pc. First, the OH, C¹⁸O, and NH₃ maps show that the dependence of column density on size is much steeper ($N \propto R^{-0.9}$) inside R_{coh} than outside of it ($N \propto R^{-0.2}$), which implies that the volume filling factor of coherent cores is much larger than in their surroundings. Second, Larson (1995) has recently found a break in the power law characterizing the clustering of stars in Taurus at 0.04 pc, just inside of R_{coh} . Larson and we interpret this break in slope as the point at which stellar clustering properties change from being determined by the (fractal) gas distribution (on scales greater than 0.04 pc) to being determined by fragmentation processes within coherent cores (on scales less than 0.04 pc).

We speculate that the transition to coherence takes place when a dissipation threshold for the MHD turbulence that characterizes the larger scale medium is crossed at the critical inner scale R_{coh} . We suggest that the most likely explanation for this threshold is the marked decline in the coupling of the magnetic field to gas motions due to a decreased ion/neutral ratio in dense, high filling factor gas.

Subject headings: ISM: clouds — ISM: kinematics and dynamics — ISM: structure — line: profiles



“Coherent Cores,” proposed in 1998

Is there a transition to a “thermal” regime? Does gravity matter more there?

THE ASTROPHYSICAL JOURNAL, 504:223–246, 1998 September 1
© 1998. The American Astronomical Society. All rights reserved. Printed in U.S.A.

COHERENCE IN DENSE CORES. II. THE TRANSITION TO COHERENCE

ALYSSA A. GOODMAN¹

Harvard University Department of Astronomy, Cambridge, MA 02138; agoodman@cfa.harvard.edu

JOSEPH A. BARRANCO

Astronomy Department, University of California, Berkeley, Berkeley, CA 94720; barranco@ucbast.berkeley.edu

DAVID J. WILNER

Harvard-Smithsonian Center for Astrophysics, 60 Garden Street, Cambridge, MA 02138; dwilner@cfa.harvard.edu

AND

MARK H. HEYER

Five College Radio Astronomy Observatory, University of Massachusetts, Amherst, MA 01003; heyer@fcrao1.phast.umass.edu

Received 1997 June 17; accepted 1998 February 5

ABSTRACT

After studying how line width depends on spatial scale in low-mass star-forming regions, we propose that “dense cores” (Myers & Benson 1983) represent an inner scale of a self-similar process that characterizes larger scale molecular clouds.

In the process of coming to this conclusion, we define four distinct types of line width–size relation ($\Delta v \propto R^a$), which have power-law slopes a_1 , a_2 , a_3 , and a_4 , as follows: Type 1—multitracer, multicloud intercomparison; Type 2—single-tracer, multicloud intercomparison; Type 3—multitracer study of a single cloud; and Type 4—single-tracer study of a single cloud. Type 1 studies (of which Larson 1981 is the seminal example) are compendia of Type 3 studies which illustrate the range of variation in the line width–size relation from one region to another.

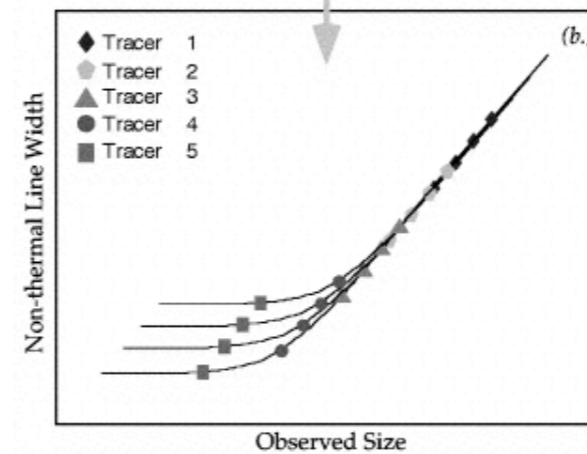
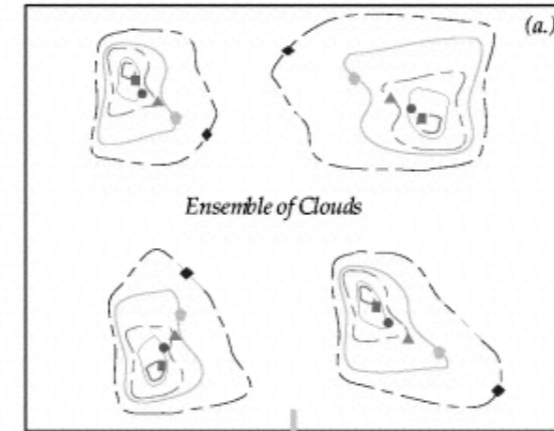
Using new measurements of the OH and C¹⁸O emission emanating from the environs of several of the dense cores studied in NH₃ by Barranco & Goodman (1998; Paper I), we show that line width increases with size outside the cores with $a_4 \sim 0.2$. On scales larger than those traced by C¹⁸O or OH, ¹²CO and ¹³CO observations indicate that a_4 increases to ~ 0.5 (Heyer & Schloerb 1997). By contrast, within the half-power contour of the NH₃ emission from the cores, line width is virtually constant, with $a_4 \sim 0$. We interpret the correlation between increasing density and decreasing Type 4 power-law slope as a “transition to coherence.” Our data indicate that the radius R_{coh} at which the gas becomes coherent (i.e., $a_4 \rightarrow 0$) is of order 0.1 pc in regions forming primarily low-mass stars. The value of the nonthermal line width at which “coherence” is established is always less than but still of order of the thermal line width of H₂. Thus coherent cores are similar to, but not exactly the same as, isothermal balls of gas.

Two other results bolster our proposal that a transition to coherence takes place at ~ 0.1 pc. First, the OH, C¹⁸O, and NH₃ maps show that the dependence of column density on size is much steeper ($N \propto R^{-0.9}$) inside R_{coh} than outside of it ($N \propto R^{-0.2}$), which implies that the volume filling factor of coherent cores is much larger than in their surroundings. Second, Larson (1995) has recently found a break in the power law characterizing the clustering of stars in Taurus at 0.04 pc, just inside of R_{coh} . Larson and we interpret this break in slope as the point at which stellar clustering properties change from being determined by the (fractal) gas distribution (on scales greater than 0.04 pc) to being determined by fragmentation processes within coherent cores (on scales less than 0.04 pc).

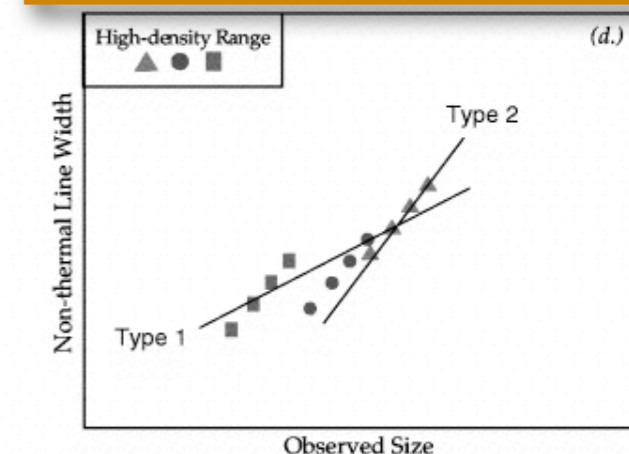
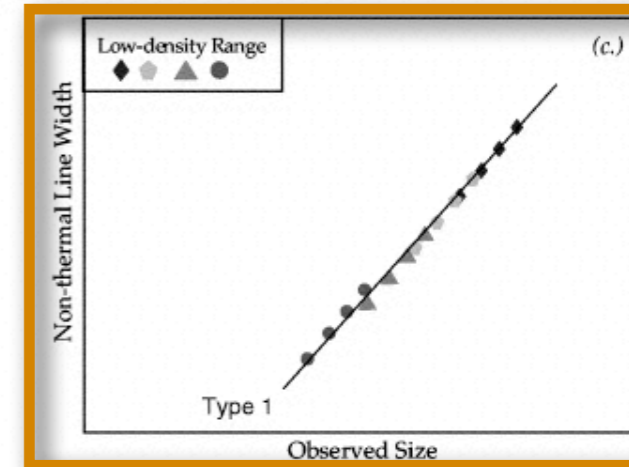
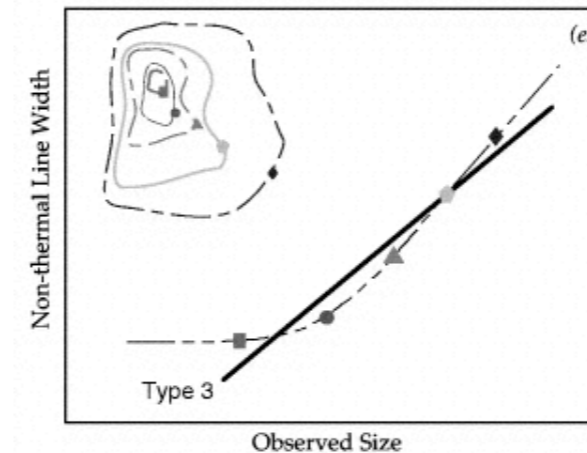
We speculate that the transition to coherence takes place when a dissipation threshold for the MHD turbulence that characterizes the larger scale medium is crossed at the critical inner scale R_{coh} . We suggest that the most likely explanation for this threshold is the marked decline in the coupling of the magnetic field to gas motions due to a decreased ion/neutral ratio in dense, high filling factor gas.

Subject headings: ISM: clouds — ISM: kinematics and dynamics — ISM: structure — line: profiles

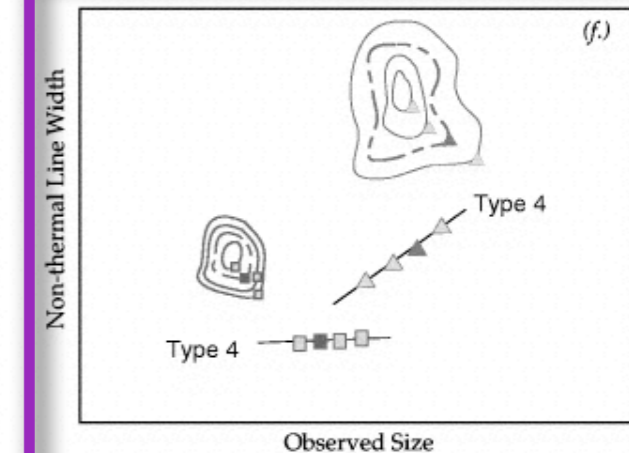
MULTIPLE CLOUDS OBSERVED IN MULTIPLE TRACERS



SINGLE CLOUD OBSERVED IN MULTIPLE TRACERS

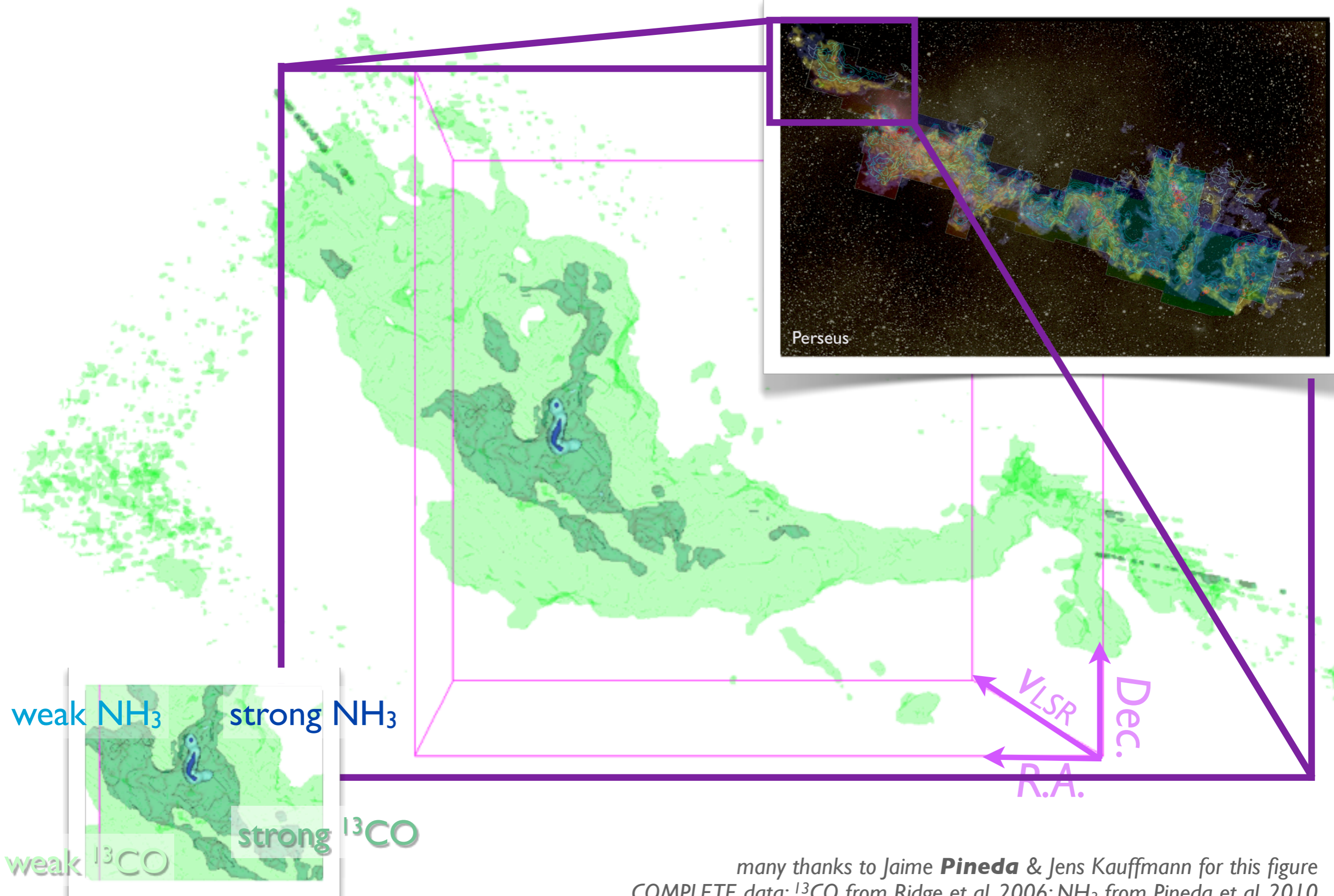


SINGLE CLOUD OBSERVED IN SINGLE TRACERS



“Coherent Cores,” proposed in 1998

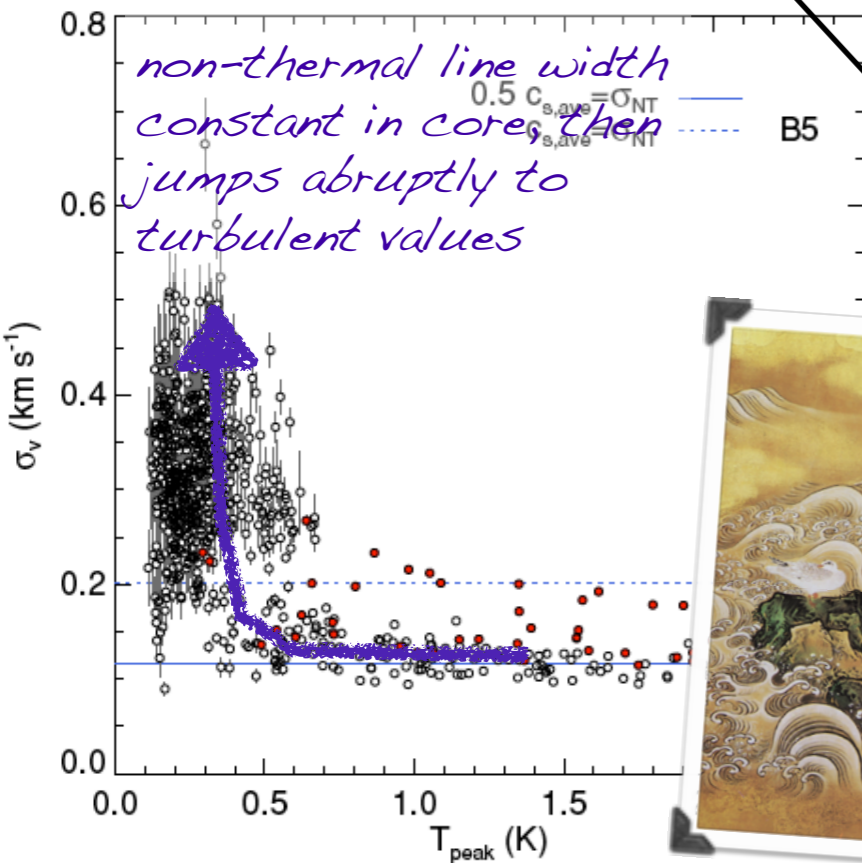
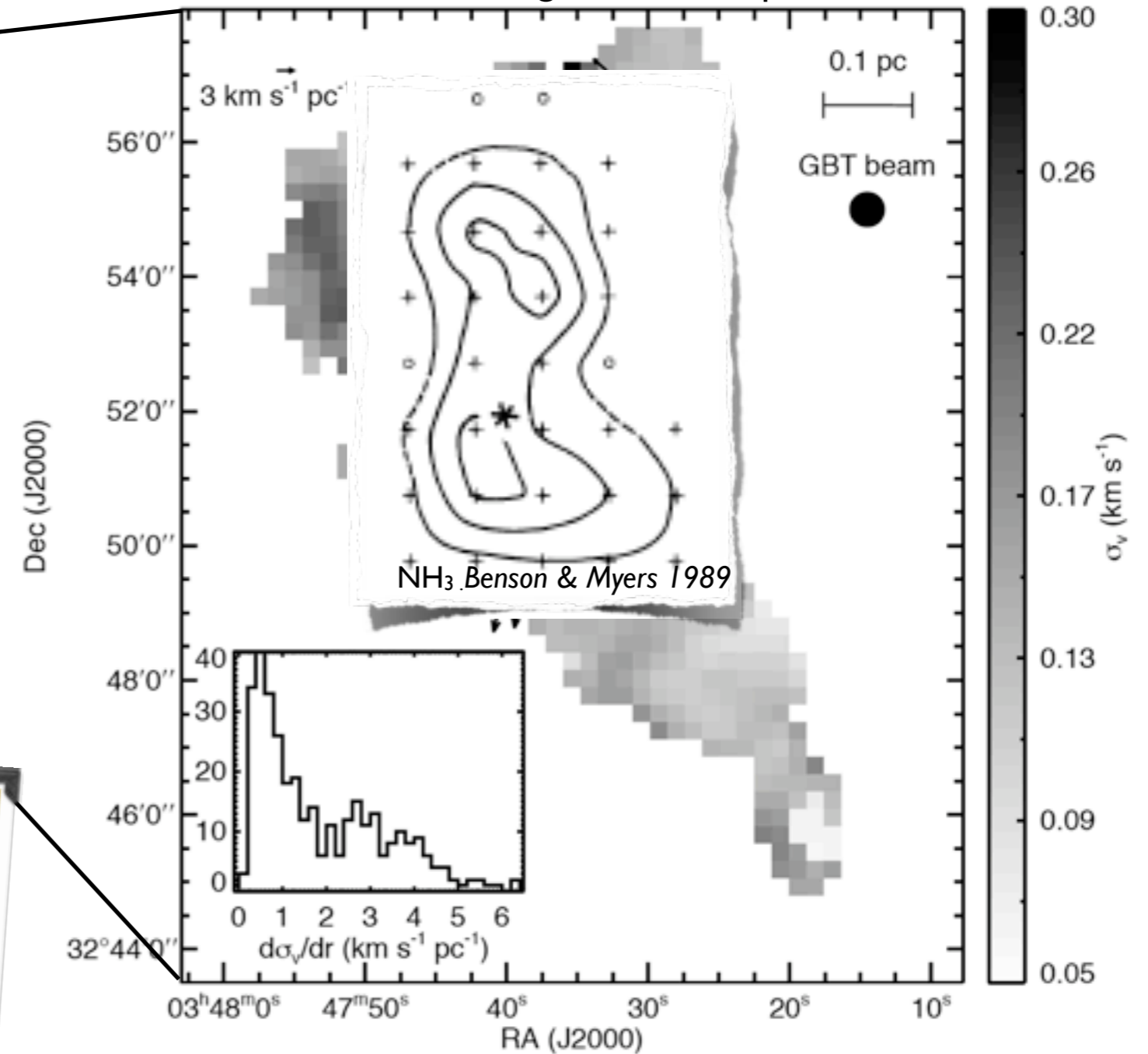
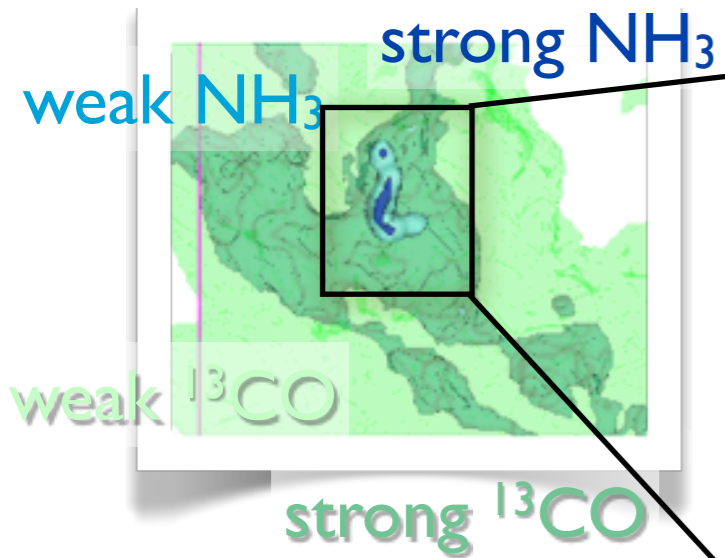
p-p-v structure of the B5 region in Perseus



many thanks to Jaime **Pineda** & Jens Kauffmann for this figure
COMPLETE data: ^{13}CO from Ridge et al. 2006; NH_3 from Pineda et al. 2010

STRONG Evidence for Coherence in Dense Cores

greyscale shows NH_3 velocity dispersion, arrows show gradient in dispersion



GBT NH_3 observations of the B5 core (Pineda et al. 2010)

Fragmentation in Coherent Cores?!

THE ASTROPHYSICAL JOURNAL LETTERS, 739:L2 (5pp), 2011 September 20

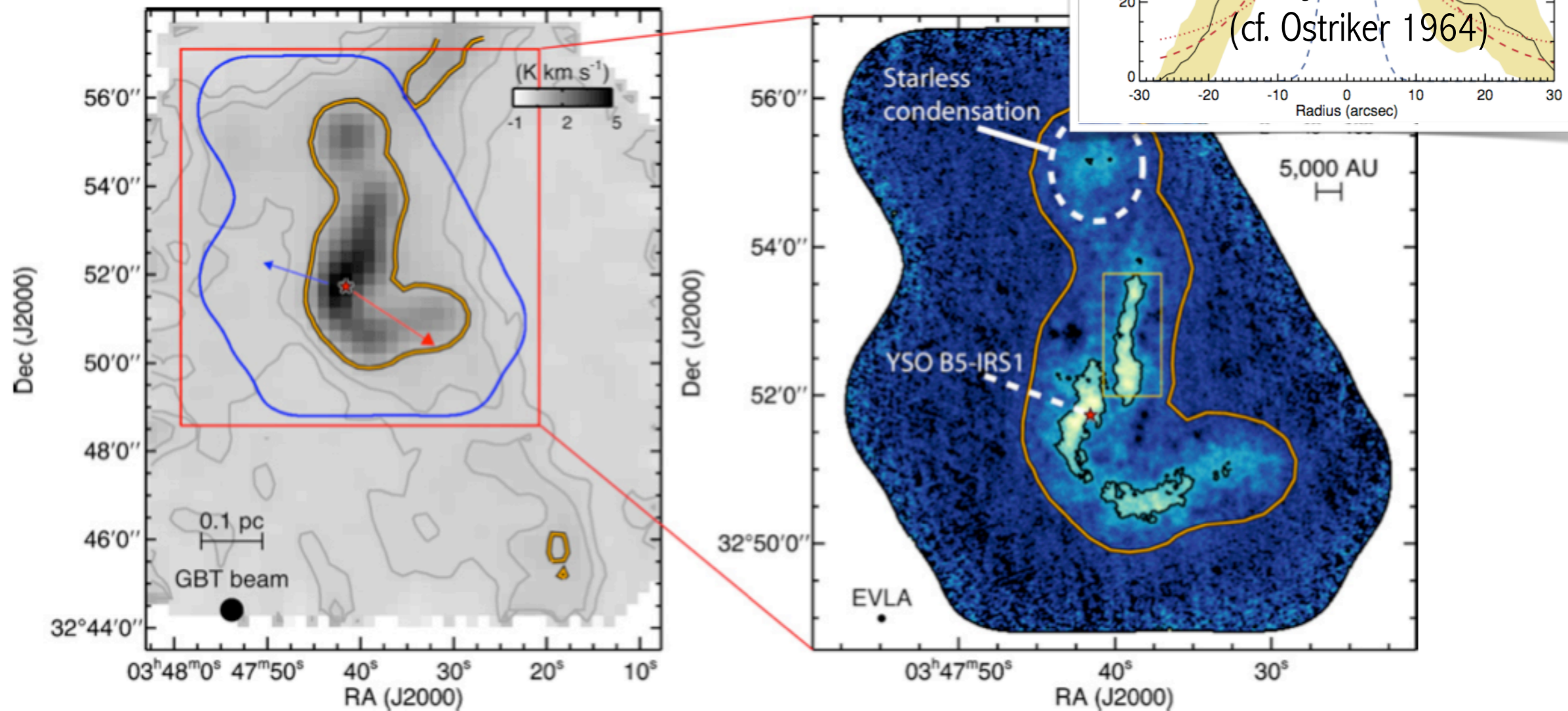
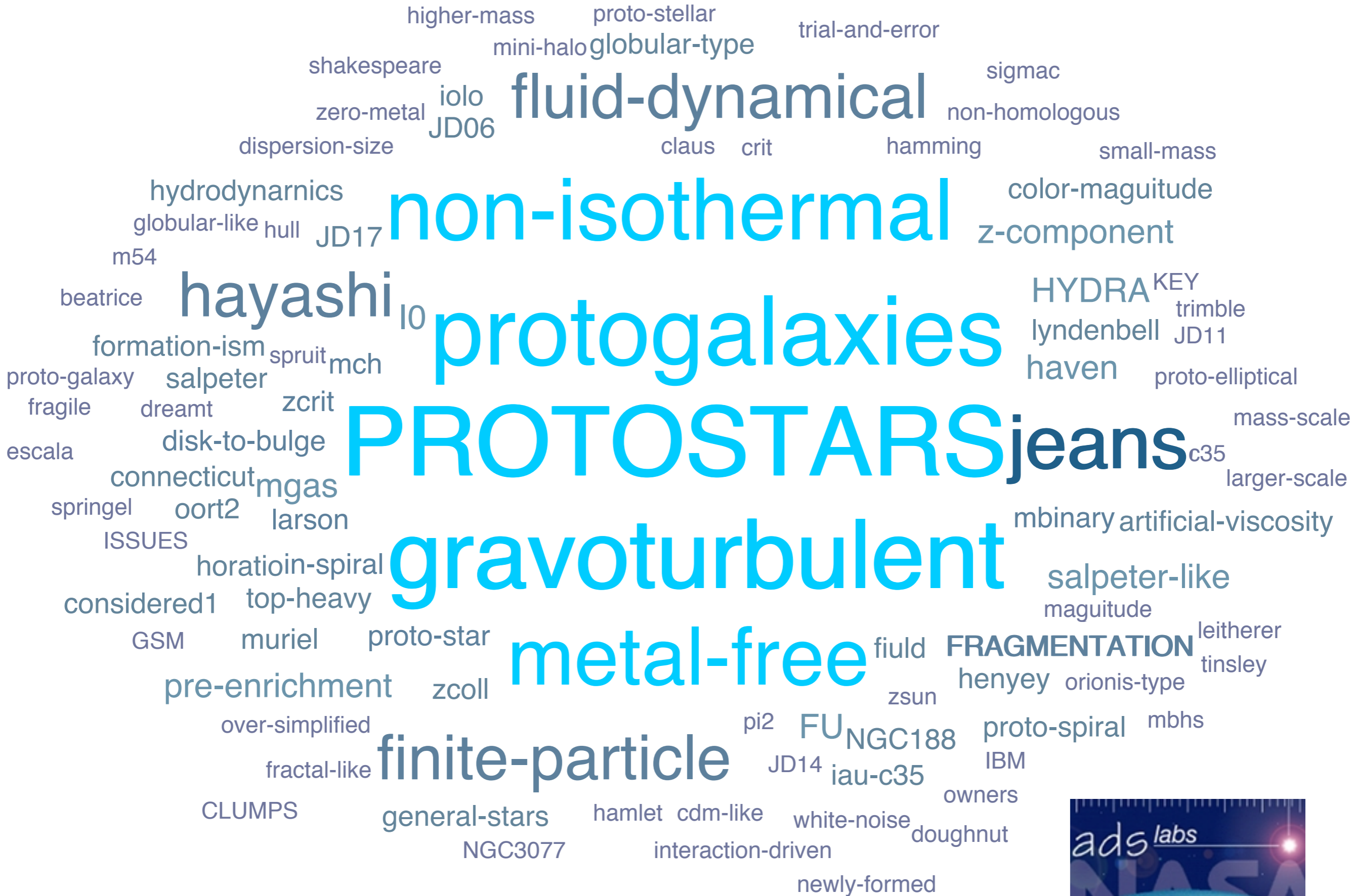


Figure 1. Left panel: integrated intensity map of B5 in NH₃ (1,1) obtained with GBT. Gray contours show the 0.15 and 0.3 K km s⁻¹ level in NH₃ (1,1) integrated intensity. The orange contours show the region in the GBT data where the non-thermal velocity dispersion is subsonic. The young star, B5-IRS1, is shown by the star in both panels. The outflow direction is shown by the arrows. The blue contour shows the area observed with the EVLA and the red box shows the area shown in the right panel. Right panel: integrated intensity map of B5 in NH₃ (1,1) obtained combining the EVLA and GBT data. Black contour shows the 50 mJy beam⁻¹ km s⁻¹ level in NH₃ (1,1) integrated intensity. The yellow box shows the region used in Figure 4. The northern starless condensation is shown by the dashed circle.

Pineda et al. 2011

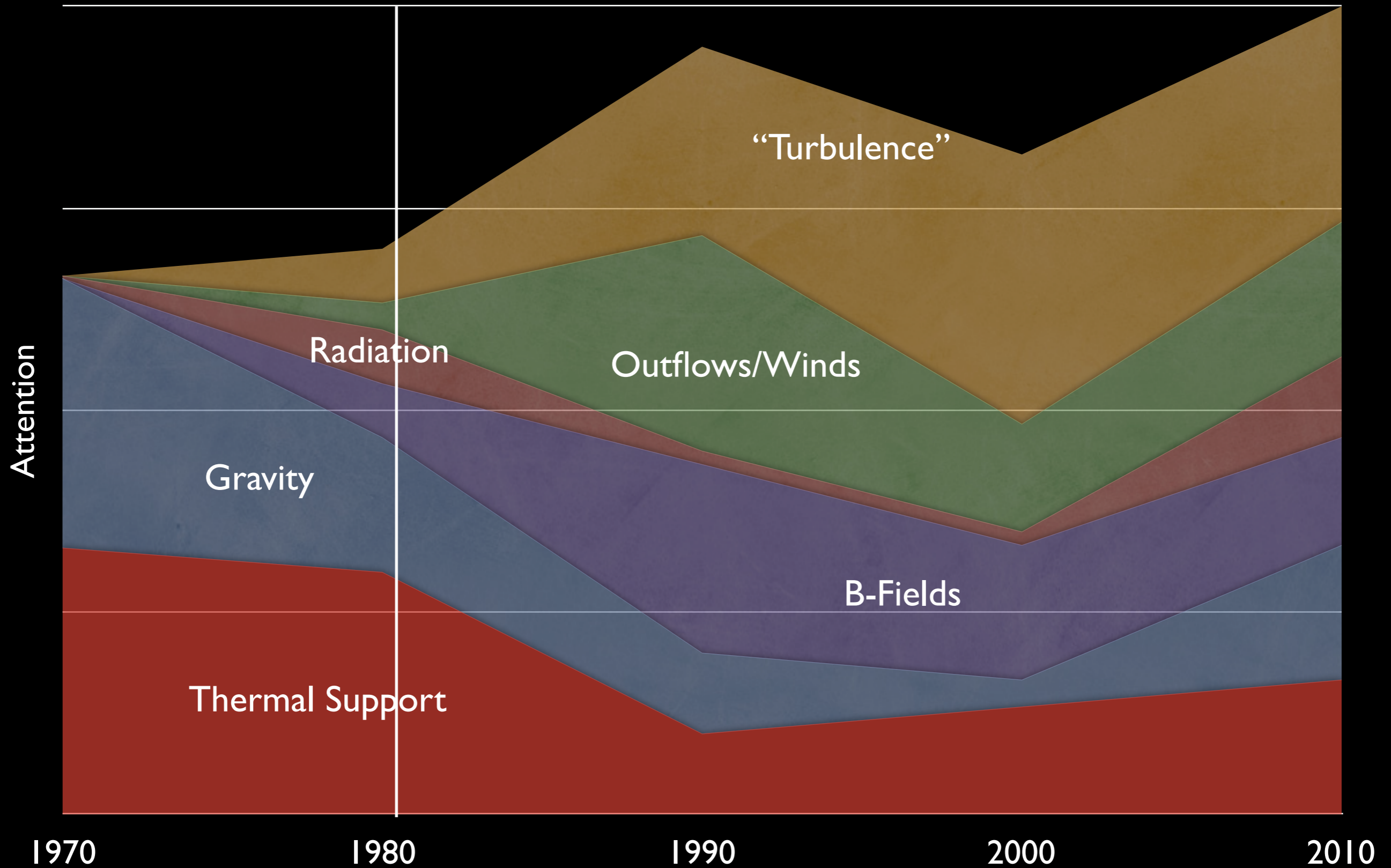
Star Formation, According to Larson (401?)



PROTOSTARS jeans, gravoturbulent

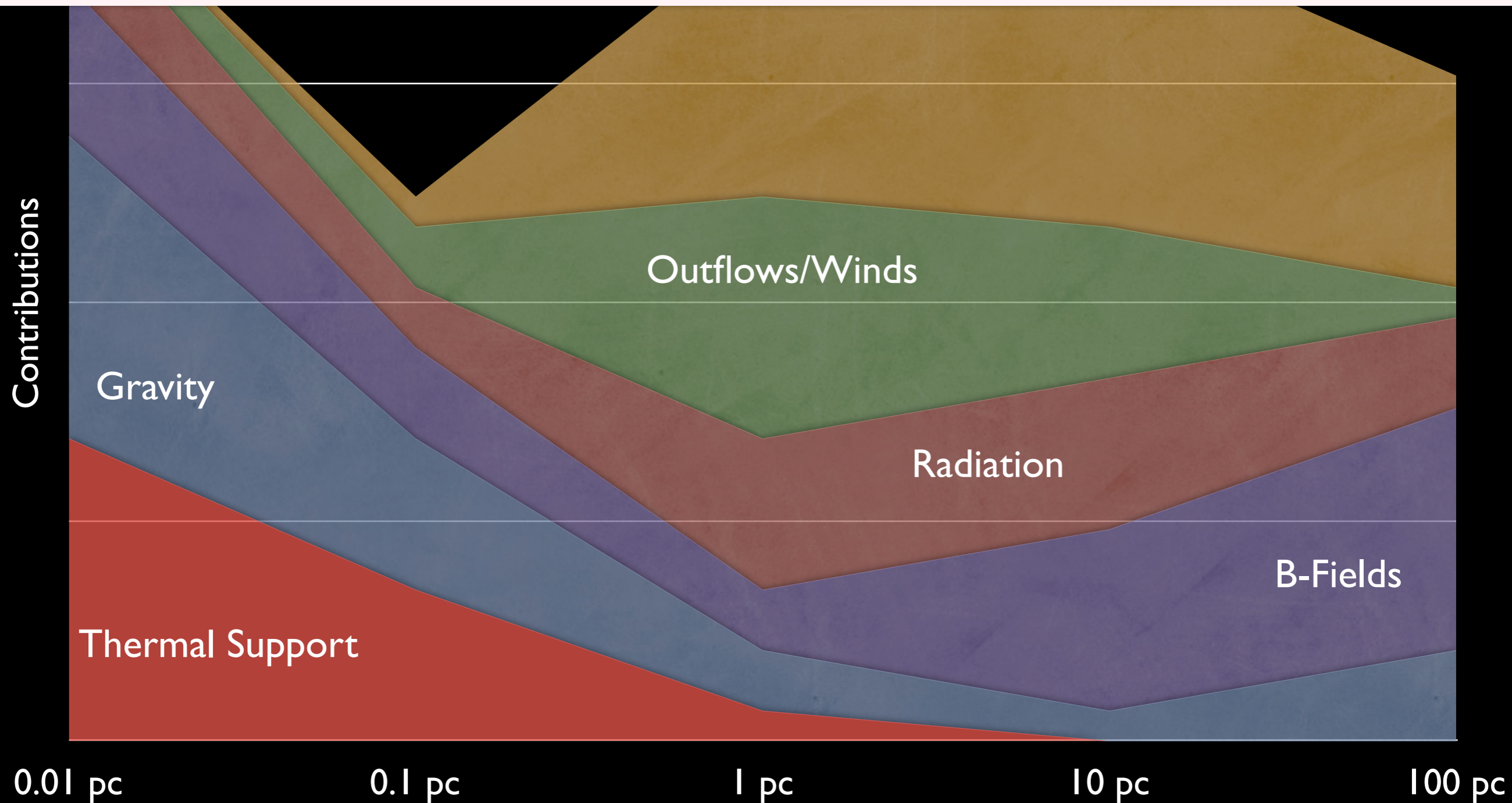
FRAGMENTATION

Changes of Heart, rather than in Physics...



What forces matter most on what scales?

Warning to Theorists:
This is a schematic, philosophical diagram!



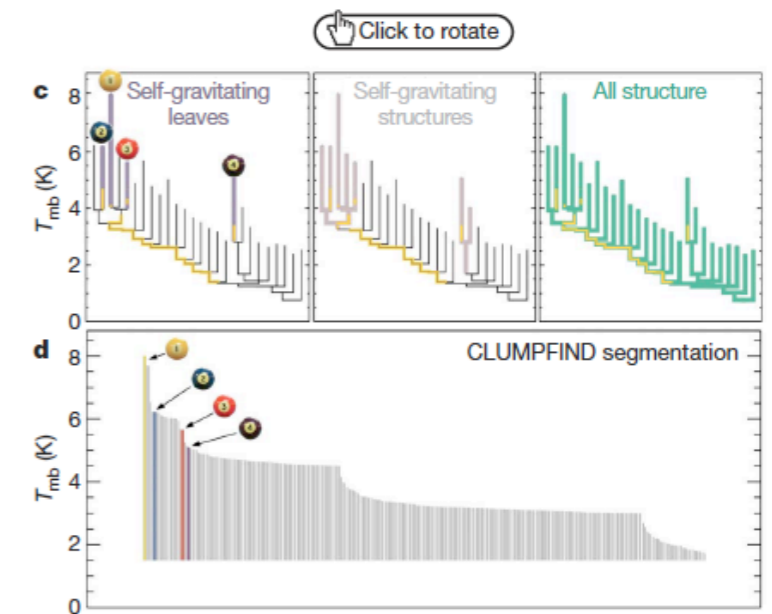
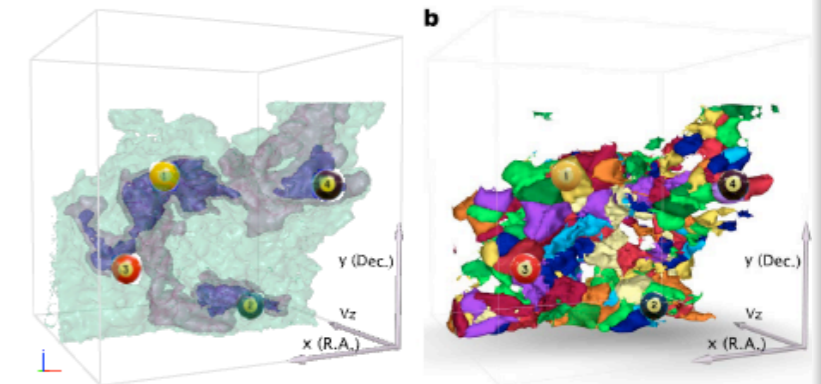
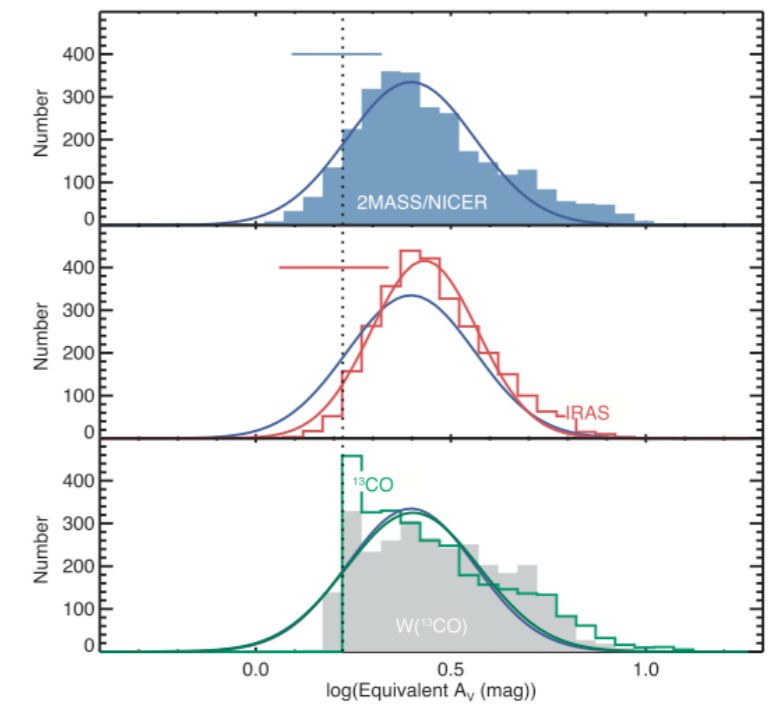
My best guess...

Gravity matters plenty in making GMCs.

Turbulent fragmentation (~no gravity necessary) is a good bet on intermediate scales (where density distribution is lognormal).

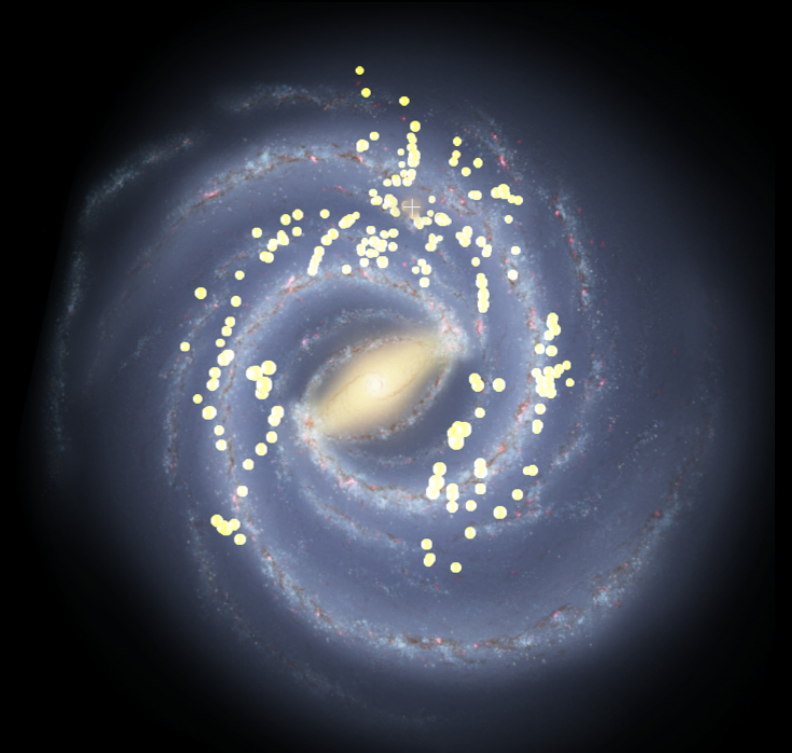
Gravity matters again on small scales, in clusters and coherent cores, and Jeans fragmentation applies here.

Magnetic fields slow things down, a little.



Goodman et al. 2009a,b

Under Pressure



Alyssa **Goodman**, Chris **Beaumont**, Tom Dame, Chris **Faesi**, Stella **Offner**, Mark Reid & Tom **Rice** (Harvard-Smithsonian Center For Astrophysics) & Joao Alves (U.Vienna), Bob Benjamin (U.Wisconsin), Erik Rosolowsky (U. British Columbia)

